energies

MDPI

Article

Anode Chamber Effluent of a Microbial Fuel Cell as a Sustainable Environment for the Cultivation of the Biohydrogen-Producing Microalga *Tetraselmis subcordiformis*

Marcin Zieliński [1,*], Marta Kisielewska [1], Paulina Rusanowska [1], Joanna Kazimierowicz [2] and Marcin Dębowski [1]

[1] Department of Environment Engineering, Faculty of Geoengineering, University of Warmia and Mazury in Olsztyn, Str. Oczapowskiego 5, 10-719 Olsztyn, Poland; jedrzejewska@uwm.edu.pl (M.K.); paulina.jaranowska@uwm.edu.pl (P.R.); marcin.debowski@uwm.edu.pl (M.D.)

[2] Department of Water Supply and Sewage Systems, Faculty of Civil Engineering and Environmental Sciences, Bialystok University of Technology, Str. Wiejska 45A, 15-351 Bialystok, Poland; j.kazimierowicz@pb.edu.pl

* Correspondence: marcin.zielinski@uwm.edu.pl

Abstract

This study evaluated the feasibility of using effluent from the anodic chamber of a microbial fuel cell (MFC), powered by real fruit and vegetable wastewater, as a cultivation medium for *Tetraselmis subcordiformis*, a microalga capable of bio-photolytic hydrogen production. In three experimental variants, different organic loading rates were applied in the anodic chamber, resulting in significant differences in effluent quality and its suitability as a culture medium. In contrast to the dominant MFC configurations, in which microalgae act as cathodic biocatalysts, the microbial fuel cell in this study was used as a source of the inevitable anode effluent, which was subsequently valorized as a cultivation medium for the marine microalga *T. subcordiformis* to support biomass and hydrogen production. In variants with moderate COD concentration and low lipid content, the highest biomass concentrations, ranging from 941 ± 104 mg VS/L to 1020 ± 108 mg VS/L, were obtained, along with the highest nitrogen assimilation efficiency (48.7–49.1%) and phosphorus assimilation efficiency (62.3–63.1%). The variant in which the culture medium contained the highest concentrations of COD, TSS, and lipids showed a substantial limitation of biomass growth to 745 ± 75 mg VS/L and lower nutrient removal efficiency (total nitrogen—42.3 ± 4.7%, total phosphorus—55.0 ± 5.0%). The obtained biomass was then used for H_2 production in a mineral photobiolytic medium. The highest total hydrogen production reached 184.7 ± 25.0 mL, while the specific hydrogen yield reached 193.7 ± 32.6 mL/g VS. Increased concentration of organic matter in the medium reduced total hydrogen production to 112.0 ± 14.8 mL, mainly due to lower biomass concentration, although the specific hydrogen yield remained high (153.4 ± 25.8 mL/g VS). The biogas composition was stable (H_2 58.0–58.7%, CO_2 35.3–35.9%, O_2 6.0–6.2%).

Keywords: *Tetraselmis subcordiformis*; MFC anodic effluent; microalgal biomass; biohydrogen; nutrient assimilation; bioenergy systems

Check for updates

Academic Editors: Alok Kumar Patel and Volodymyr Shentsov

Received: 12 December 2025
Revised: 3 February 2026
Accepted: 6 February 2026
Published: 8 February 2026

Copyright: © 2026 by the authors. Licensee MDPI, Basel, Switzerland. This article is an open access article distributed under the terms and conditions of the Creative Commons Attribution (CC BY) license.

1. Introduction

The energy transition towards a low-emission economy requires the implementation of technologies that enable the simultaneous acquisition of energy from renewable resources and waste, thereby reducing emissions and lowering the environmental burden associated

with pollution streams [1]. In this context, bioenergy systems are becoming increasingly important, as they allow the transformation of biodegradable wastes of various characteristics and origins into gaseous, liquid, and solid energy carriers [2]. Due to their ability to directly generate electrical current, microbial fuel cells (MFCs) represent a competitive and promising solution compared with conventional technologies. They are a class of bioelectrochemical systems in which microorganisms convert the chemical energy of organic substrates into electrical energy while simultaneously removing pollutants introduced into the system [3].

Particular attention is given to solutions that integrate MFCs with photoautotrophic microalgal biomass, which can function as an autotrophic biocatalyst supplying oxygen to the cathodic chamber, thereby eliminating the need for external aeration and stabilising the electrode potential [4–6]. In other technological configurations, MFC–PBR (photobioreactor) integration is based on the use of mineralised effluent originating from the anaerobic anodic chamber of the MFC [7–9].

Available studies indicate that microalgal species from freshwater environments exhibit higher effectiveness in MFC biocathodes than marine species, which is linked to the physicochemical properties of the medium, including lower electrolyte conductivity, reduced risk of parasitic ionic flows, and more favourable reagent diffusion across ion-exchange membranes [10]. Increased salinity of the culture medium, characteristic of marine microalgal species, destabilises bioelectrochemical processes due to the rise in electrolyte conductivity and intensification of parasitic ionic shunt currents, which lead to energy losses and disturbances in charge transport [11]. As a result, the use of marine microalgae in the cathodic chamber of MFCs is technologically limited and does not favour high electrical energy generation efficiency [12]. On the other hand, many marine species exhibit high biomass growth dynamics, favourable sedimentation properties, strong adaptive capacity to difficult and variable environmental conditions, and potential for producing multiple energy carriers [13].

Despite the intensive development of MFC systems, an alternative and increasingly explored strategy for integrating anaerobic technologies with microalgae is the use of effluents from anaerobic digestion reactors (e.g., UASB, CSTR, AnMBR) as a source of nutrients and carbon for microalgal cultivation [14]. In this approach, microalgae do not serve as an electrochemical component; instead, they constitute a platform for nitrogen and phosphorus recovery, reduction in residual organic matter, and production of valuable biomass [15]. Importantly, post-anaerobic effluents are streams that in practice require further treatment prior to discharge to the environment, and their valorization in microalgal cultivation enables simultaneous reduction in pollutant concentrations and resource recovery in line with the circular economy concept [16]. A similar concept may be extended to the bioelectrochemical MFC stage, where the anode chamber effluent is treated as a stream requiring further management and can be transformed into a cultivation medium for microalgae and subsequently used to obtain value-added products.

One species with significant bioenergy potential is *Tetraselmis subcordiformis* (*T. subcordiformis*), a eurybiotic unicellular green alga capable of synthesising metabolites of biofuel importance, including precursors for biogas production [17], bio-oil [18], and biohydrogen [19]. The marine nature of this taxon, however, limits its applicability in MFC biocathodes, although it potentially enables its use in integrated systems in which the culture medium is derived from effluent streams from the anodic chamber of an MFC [20].

From a circular economy perspective, it is particularly important to use biodegradable waste from the food industry as anodic substrates, including fruit and vegetable wastewater [21]. Such waste, after anaerobic fermentation, generates effluents rich in nitrogen, phosphorus, and simple, biologically available organic compounds, which may potentially

support mixotrophic microalgal growth [22,23]. The literature shows that by-products of anaerobic degradation processes can serve as nutrient sources for microalgae, including *T. subcordiformis* [24]. However, no studies have reported the use of effluents from the anodic chamber of an MFC supplied with real fruit and vegetable wastewater as a culture medium for this species. There is also no information regarding the effects of such effluents on biomass growth kinetics, population density, biochemical properties of the microalgae, their hydrogen-producing capacity, or the quality of the resulting biogas.

The literature is dominated by integrated MFC systems, in which microalgae act as an oxygen source and biocatalyst in the cathode chamber, and research objectives primarily focus on improving the electrochemical performance of the device. In the present study, a different approach was adopted. The MFC was primarily considered as a module for preliminary bio-processing of wastewater streams from the fruit and vegetable processing sector, while the anode chamber effluent, inevitably generated during operation, was subsequently valorized as a cultivation medium. Particular emphasis was placed on the use of the marine microalga *T. subcordiformis*, whose salinity requirements limit its application in conventional MFC biocathodes, yet support the concept of valorizing anode effluents toward biomass and hydrogen production. The above highlights a research gap regarding the bioelectrochemical–photobiological integration of MFC systems with the cultivation of *T. subcordiformis* using waste resources from fruit and vegetable processing.

This study aims to assess the suitability of effluents from the anodic chamber of an MFC powered by fruit and vegetable wastewater at different organic loading rates as a culture medium for *T. subcordiformis*, and to determine their effects on biomass production efficiency, population growth kinetics, biochemical properties of the obtained biomass, and the parameters and efficiency of biological hydrogen production, as well as the qualitative characteristics of the generated biogas. The study tested the hypothesis that effluents from the anodic chamber of an MFC can serve as a functional culture medium for *T. subcordiformis*, and that their composition, determined by the applied organic loading rate, will influence both the intensity of microalgal growth and their bioenergy potential for hydrogen production.

2. Materials and Methods

2.1. Experimental Organisation

The experimental work was divided into two stages (S). In the first stage (S1), the biomass production efficiency of *T. subcordiformis* and the nutrient utilisation efficiency by the microalgae were analysed. After cultivation, the biomass was separated from the culture medium and concentrated by sedimentation. The final concentration of microalgae in the photobioreactors (PBR) was then determined, and analyses were conducted to characterise the composition of the obtained biomass. The second stage (S2) involved hydrogen production by *T. subcordiformis* in respirometric reactors. The microalgae were incubated in a medium providing optimal conditions for biophotolytic processes in respirometric reactors, where the volume of produced gas was monitored, along with qualitative analysis of hydrogen content.

In each stage, three variants (V) were distinguished. The criterion for their separation was the applied organic loading rate (OLR) in the anodic chamber of the microbial fuel cell (MFC), which was supplied with fruit and vegetable wastewater. The OLR values in the experimental variants were: 1.0 g COD/L·d (V1), 2.0 g COD/L·d (V2), and 3.0 g COD/L·d (V3). These variants constituted a technological criterion enabling evaluation of how the degree of loading in the anodic chamber influenced the composition and properties of the effluents used as a cultivation medium for *T. subcordiformis*, as well as their impact

on biomass production efficiency (S1) and hydrogen generation (S2). The organisational scheme of the experimental workflow is presented in Figure 1.

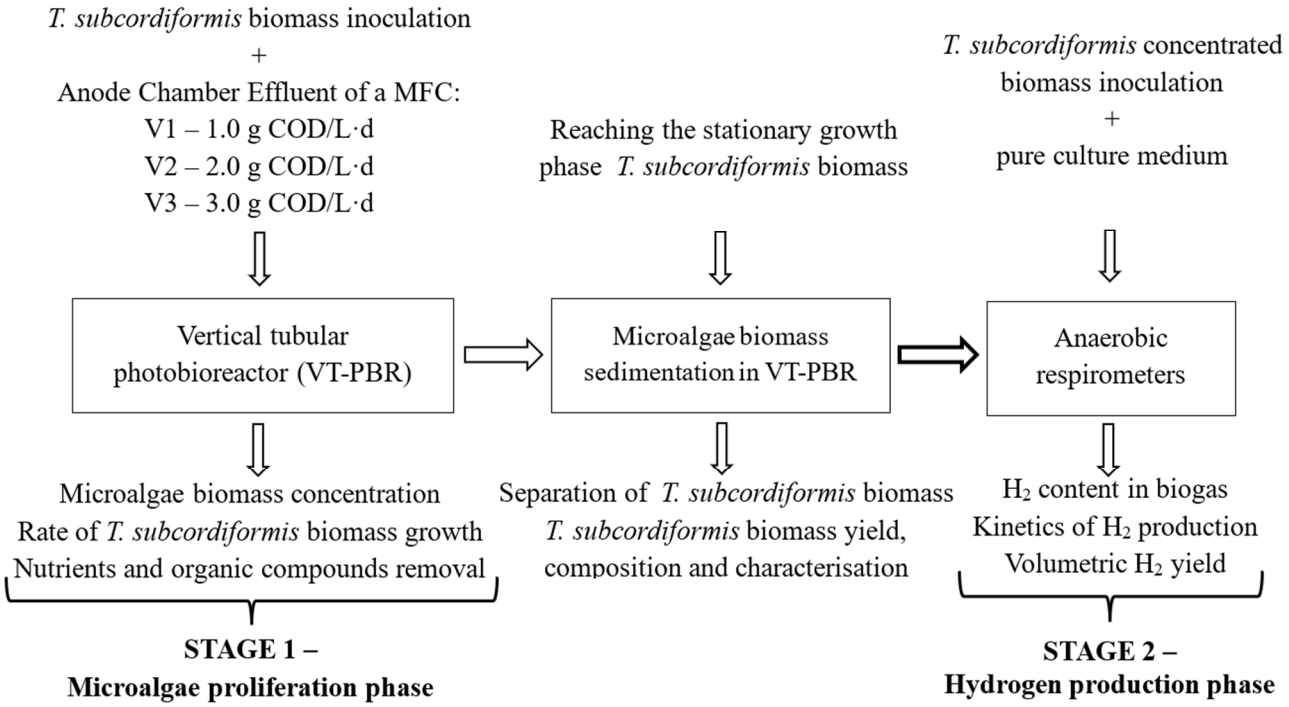


Figure 1. Organisation and planned sequence of the experimental work.

2.2. Materials

2.2.1. Inoculum of *T. subcordiformis*

Cultures of the microalga *T. subcordiformis* (strain SAG 161-1a) were obtained from the algal collection of the University of Göttingen (Göttingen Germany), operating under the international abbreviation SAG. In the initial cultivation phase, the inoculum was propagated to obtain sufficient biomass for the experiment, using a culture medium prepared from chemical reagents [25]. The culture was first maintained in sterile glass tubes with a working volume of 50 mL (Biospace, Poznań, Poland). Once sta, le cultures were established, they were transferred to glass bioreactors with a capacity of 1.0 L (Duran Bottle System, Mainz, Germany). All laboratory glassware was sterilised in an autoclave (2840 EL-D, Tuttnauer, New York, NY, USA) at 121 °C for 15 min.

2.2.2. Fruit and Vegetable Wastewater and Culture Media

In S1, the PBRs were inoculated with effluent from the anodic chamber of the microbial fuel cell (MFC), where anaerobic biodegradation of contaminants from real fruit and vegetable wastewater was performed by fermentative microorganisms. Raw wastewater was obtained from a fruit and vegetable processing plant (Maspex Sp. z o.o., KUBUŚ Juice Production Plant, Olsztynek, Poland). The characteristics of the wastewater used to supply the anaerobic anodic chamber of the MFC are shown in Table 1.

The anaerobic anodic chamber was a completely mixed system with a working volume of 1.0 L and operated at a temperature of 35–37 °C. Anaerobic microorganisms were immobilised as a biofilm on a conductive carbon cloth with a surface area of approximately 30 cm^2. The anaerobic sludge used in this study represented a natural microbial consortium typical of methanogenic environments, comprising functional groups responsible for successive stages of anaerobic biodegradation of organic matter. These included hydrolytic and fermentative bacteria converting complex substrates into VFAs and alcohols (repre-

sentatives of *Firmicutes* and *Bacteroidota*), syntrophic bacteria oxidising VFAs and alcohols in cooperation with hydrogen-consuming microorganisms (*Syntrophomonas*, *Syntrophobacter*), and methanogenic archaea utilising acetate and hydrogen (*Methanosaeta/Methanothrix*, *Methanosarcina*, *Methanobacterium*). After stable electrochemical activity was achieved, the system was operated under three OLR levels: V1—1.0 g COD/L·d, V2—2.0 g COD/L·d, and V3—3.0 g COD/L·d. Depending on the selected organic loading rate, the hydraulic retention time (HRT) in the anaerobic anodic chamber varied (V1—8.4 days, V2—4.2 days, V3—2.8 days). The applied technological parameters significantly affected the quality of the effluent from the MFC anodic chamber, which served as the culture medium for *T. subcordiformis* biomass production in S1 (Table 2).

Table 1. Characteristics of real fruit and vegetable wastewater supplied to the MFC anodic chamber.

Parameter	Unit	Value (Mean ± SD)
COD	mg O_2/L	8400 ± 4032
BOD_5	mg O_2/L	5040 ± 2688
TSS	mg/L	2700 ± 1600
pH	–	6.7 ± 0.8
Soluble sugars	mg/L	4200 ± 2300
TN (total nitrogen)	mg N/L	249 ± 120
NH_4^+-N	mg N/L	53 ± 35
TP (total phosphorus)	mg P/L	27 ± 17
P-PO_4	mg P/L	18 ± 6.2
Lipids	mg/L	135 ± 85
Conductivity	mS/cm	11.8 ± 4.7

Table 2. Characteristics of the effluent from the MFC anodic chamber used as the culture medium in the experimental variants.

Parameter	Unit	V1—1.0 g COD/L·d (HRT 8.4 Days)	V2—2.0 g COD/L·d (HRT 4.2 Days)	V3—3.0 g COD/L·d (HRT 2.8 Days)
COD	mg O_2/L	2100 ± 1010	2250 ± 1150	3200 ± 1460
BOD_5	mg O_2/L	504 ± 250	540 ± 270	800 ± 380
TSS	mg/L	1080 ± 330	1120 ± 420	1550 ± 450
pH	–	6.9 ± 0.3	6.88 ± 0.33	6.7 ± 0.5
Soluble sugars	mg/L	125 ± 85	140 ± 92	154 ± 77
TN	mg N/L	217 ± 111	215 ± 106	226 ± 115
NH_4^+-N	mg N/L	100 ± 50	110 ± 55	130 ± 65
TP	mg P/L	22 ± 11	22.5 ± 12	25 ± 12
P-PO_4	mg P/L	13 ± 2	14 ± 3	14 ± 3
Lipids	mg/L	34 ± 20	36 ± 21	80 ± 43
Conductivity	mS/cm	10.5 ± 4.0	10.6 ± 4.1	11.2 ± 4.5

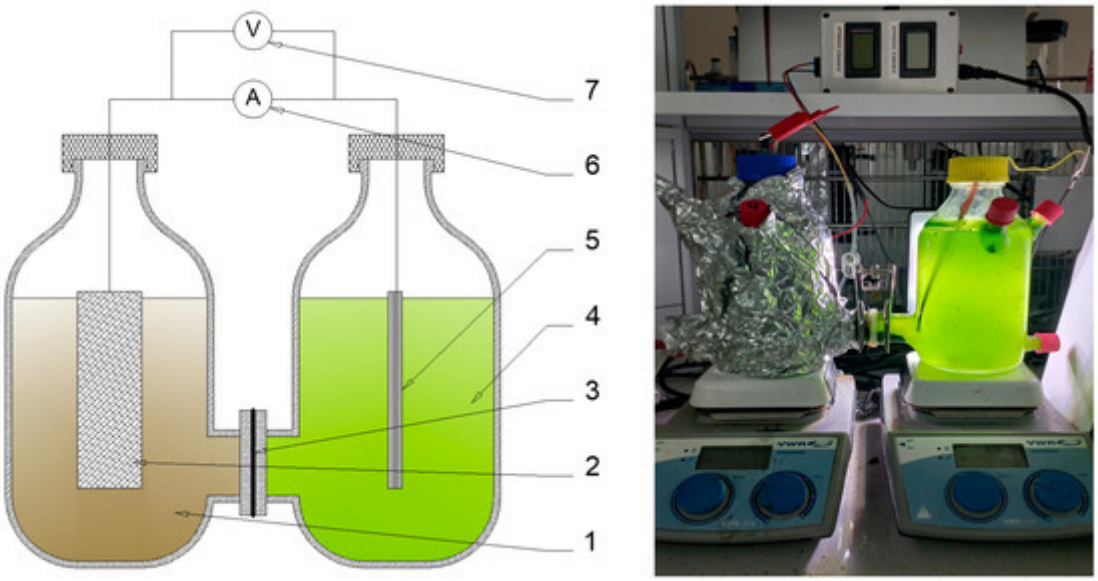
In all experimental variants in which hydrogen production efficiency (S2) was evaluated, a culture medium based on deionised water was used, enriched with mineral salts and trace elements essential for proper microbial functioning. The medium contained (mg/L): $NaHCO_3$—0.196, for pH buffering; KCl—0.667 and NaCl—27.23, to ensure ionic

balance; H_3BO_3—0.098 and KBr—0.098 as sources of trace elements; $CaCl_2$—1.123 and $MgCl_2$—5.079 as components necessary for cellular metabolism; NaF—0.003, $SrCl_2$—0.024, and $CuCl_2$—0.002 as microelements supporting enzymatic biological processes. The pH of the medium was maintained between 7.90 and 8.00. The composition of the medium was developed based on available literature data and the authors' previous studies [26].

2.3. Photobioreactors

2.3.1. Cultivation of Microalgae in the Photobioreactor (S1)

T. subcordiformis was cultivated in vertical, column-type photobioreactors (VT-PBR) with an active volume of 1.0 L (Aquamedic, Janikowo, Poland) at a controlled temperature of 25 °C (Figure 2). The reactor was completely filled with effluent from the anaerobic anodic chamber of the MFC, which served as the culture medium. Subsequently, an inoculum of *T. subcordiformis* was then added at an initial concentration of 150 mg VS/L. Depending on the applied OLR in the MFC anodic chamber, the culture medium displayed different physicochemical parameters, reflecting the experimental conditions of the respective variants (Table 2). The PBR was illuminated using 10 W white lamps (Leddy Slim, Aquael, Warsaw, Poland) with a colour temperature of 900 K. The photon flux in the PAR range (400–700 nm) was 270–300 µmol/m^2 s, corresponding to 720 lm. Air was supplied using Hailea V10 pumps (Hailea Group, Chaozhou, China) with a capacity of 200 L/h, ensuring medium mixing and aeration.



(**a**) (**b**)

Figure 2. Schematic diagram (**a**) and photograph (**b**) of the MFC used to obtain effluent from the anaerobic anode chamber (1—anode chamber, 2—carbon felt anode, 3—Nafion membrane, 4—cathode chamber, 5—carbon cloth cathode, 6—ammeter, 7—voltmeter). The grey colour indicates anaerobic sludge, while the green colour indicates microalgal biomass.

2.3.2. Hydrogen Production Reactor (S2)

Biomass of *T. subcordiformis* obtained from the PBR was separated by simple sedimentation and introduced into respirometric reactors (OxiTop—IDS, WTW, Weilheim, Germany) with an active volume of 1.0 L. Incubation was carried out at 25 ± 1 °C, with the reactor contents magnetically stirred at 60 rpm. The medium and the reactor headspace were deoxygenated by purging with nitrogen (N_2) at a flow rate of 100 L/h for 3 min to ensure anaerobic conditions required for hydrogenase activation. Pressure changes in the gas phase were recorded every 10 h and converted to volumetric biogas production

under standard conditions using the ideal gas law. The incubation lasted 120 h, comprising 30 h in the dark phase and 90 h in the light phase. The reactors were illuminated with daylight fluorescent lamps (Philips MASTER TL-D Super 80, Eindhoven, The Netherlands) with a colour temperature of 6500 K and a power of 58 W, simulating natural daylight conditions and supporting photosynthetic H_2 production. Initial biomass concentrations in each variant depended on the biomass yield obtained in S1, allowing assessment of the effects of different biomass yields on hydrogen production.

2.3.3. Characterisation of the Microbial Fuel Cell (MFC)

A conventional, two-chamber microbial fuel cell (MFC) operated in fed-batch mode, with an "H-type" configuration, was used in the experiments. The cell consisted of two glass bottles with a nominal volume of 1000 mL each, forming separate chambers: an anode (anaerobic) and a cathode (aerobic) chamber. The chambers were connected by a channel equipped with an ion separator in the form of a Nafion™ 117 proton-exchange membrane (Sigma-Aldrich, St. Louis, MO, USA) with dimensions of 5 cm × 5 cm, enabling ion transport (mainly H^+ and other cations) while limiting electrolyte mixing. The anode was made of conductive carbon cloth with dimensions of 5 cm × 6.0 cm and an active surface area of 30 cm^2. The cathode consisted of a carbon rod with a diameter of 0.4 cm and an active surface area of 17.84 cm^2. To improve mass transfer and maintain medium homogeneity, the contents of both chambers were mixed using magnetic stirrers. The operating temperature was maintained at 35–37 °C. The electrodes were connected via an external electrical circuit including a copper wire and a resistor (R = 100 Ω). Current and cell voltage were recorded periodically (every 2 h) using a digital multimeter with automatic range selection. A schematic of the two-chamber MFC (including chamber separation, Nafion membrane, electrodes, and the V–I measurement system) is presented in Figure 2.

The anode chamber was operated under anaerobic conditions (maintained in the dark and covered with aluminium foil), whereas the cathode chamber was run under aerobic conditions to ensure the availability of an electron acceptor at the cathode. To maintain anoxic conditions in the anode chamber, after each medium replacement the chamber was purged with a gas mixture of 80% N_2 and 20% CO_2 for 10 min. The anode chamber was inoculated with anaerobic sludge collected from the municipal wastewater treatment plant "Łyna" (Olsztyn, Poland). The sludge was introduced into the anode chamber and mixed for 24 h to allow sedimentation and immobilisation of microorganisms on the anode surface (formation of an electroactive biofilm). Subsequently, part of the sludge was removed and the chamber was fed with fresh wastewater. Anaerobic microorganisms were immobilised as a biofilm on the conductive carbon-cloth anode (≈30 cm^2). After stable electrochemical activity was achieved, the system was operated under three organic loading rate (OLR) variants, which determined the hydraulic retention time (HRT).

In the cathode chamber, a culture of *Arthrospira platensis* (UTEX 3086, Culture Collection of Algae, University of Texas, Austin, TX, USA) was applied. The inoculum was prepared by cultivation in laboratory-scale photobioreactors (2 L) in a thermostatic chamber at 35 °C prior to inoculation of the MFC system. The medium for *A. platensis* was prepared according to a modified Aiba and Ogawa medium [27]: 13.61 g $NaHCO_3$, 4.03 g Na_2CO_3, 0.5 g K_2HPO_4, 2.5 g $NaNO_3$, 1.0 g K_2SO_4, 1.0 g NaCl, 1.0 g $MgSO_4 \cdot 7H_2O$, 0.04 g $CaCl_2 \cdot 2H_2O$, 0.01 g $FeSO_4 \cdot 7H_2O$, 0.08 g Na_2EDTA, and 1 mL of A5 and B6 trace-element solutions per 1 L of distilled water. The cathode chamber was operated under a 16:8 h (light:dark) photoperiod and illuminated with white light (fluorescent lamps). During MFC operation, the *A. platensis* biomass concentration ranged from 2.0 to 4.2 g TS/L. Aeration of the cathode chamber was provided at 120 dm^3/h. The electrochemical performance of

the two-chamber MFC fed with fruit and vegetable processing wastewater under different organic loading rates (OLR) is summarised in Table 3.

Table 3. Electrochemical parameters of the two-chamber MFC fed with fruit and vegetable processing wastewater as a function of organic loading rate (OLR).

Variant	OLR (g COD/L·d)	HRT (d)	Power Density $\overline{PD}$ (mW/m^2)	Power Output $\overline{P}$ (mW)	Voltage $\overline{V}$ (mV)	Current $\overline{I}$ (mA)	Coulombic Efficiency $\overline{CE}$ (%)
V1	1.0	8.4	35 ± 5	0.098 ± 0.042	313 ± 67	0.313 ± 0.067	22 ± 8
V2	2.0	4.2	60 ± 25	0.168 ± 0.070	410 ± 85	0.410 ± 0.085	16 ± 6
V3	3.0	2.8	55 ± 30	0.154 ± 0.084	392 ± 107	0.392 ± 0.107	11 ± 5

2.4. Analytical, Computational, and Statistical Methods

The control and measurement equipment used during the experimental work, as well as the applied calculation procedures and statistical tests, are presented in Table 4.

Table 4. Measurement devices and analytical, computational, and statistical methods used.

Parameter	Method	Equipment/Manufacturer, City, Country
Volatile solids (VS)	Gravimetric determination by ignition at 550 °C	Muffle furnace LAC L, Dąbrowica, Poland; ash weighing DanLab AX423, Białystok, Poland
Taxonomic analysis	Light microscopy	Biological microscope MF 346 with Optech 3MP camera, Eduko, Warsaw, Poland
COD	Dichromate method PN-EN 12260 with sample mineralisation	Block Digest mineraliser, VELP Scientifica, Usmate, Italy; UV/VIS DR 5000 spectrophotometer, Hach Lange, Düsseldorf, Germany
BOD_5	5-day incubation	OxiTop-IDC respirometer, WTW, Weilheim, Germany; standard respirometric procedure
Total nitrogen (TN)	Kjeldahl/spectrophotometric	UV/VIS DR 5000 spectrophotometer, Hach Lange, Düsseldorf, Germany; Kjeldahl apparatus VELP Scientifica, Usmate, Italy
NH_4-N	Colorimetric	UV/VIS DR 5000 spectrophotometer, Hach Lange, Düsseldorf, Germany
Total phosphorus (TP)	Colorimetric (molybdenum method)	UV/VIS DR 5000 spectrophotometer, Hach Lange, Düsseldorf, Germany
pH	Glass electrode	pH meter 1000 L, VWR International, Radnor, PA, USA
Salinity	Conductivity electrode	Marine Control Digital, Aqua Medic, Janikowo, Poland
VS (in wastewater)	Gravimetric	Ignition in LAC L muffle furnace, Dąbrowica, Poland
Protein	Nitrogen determination (Kjeldahl) × factor 6.25	Kjeldahl apparatus VELP Scientifica, Usmate, Italy
Lipids	Soxhlet extraction/chloroform method	Soxhlet apparatus VELP Scientifica, Usmate, Italy; chloroform Sigma-Aldrich, St. Louis, MO, USA; analytical balance Sartorius Cubis, Göttingen, Germany
Sugars	Phenol-sulfuric colorimetric method	UV/VIS DR 5000 spectrophotometer, Hach Lange, Düsseldorf, Germany

Table 4. *Cont.*

Parameter	Method	Equipment/Manufacturer, City, Country
H_2, O_2, CO_2	Gas chromatography	GC Agilent 7890 A, Agilent Technologies, Santa Clara, CA, USA; samples collected with gas-tight syringe
Gas production rate (r) and kinetic constants (k)	Nonlinear (iterative) regression	–
Experimental replications	Four replicates per variant	–
Statistical analysis	–	Statistics 13.3, Statsoft, Inc., Tulsa, OK, USA
Significance level	–	$\alpha = 0.05$
Normality and homogeneity tests	–	Shapiro–Wilk test, Levene's test
Analysis of differences between means	–	One-way ANOVA and HSD (honestly significant difference) test

3. Results and Discussion

3.1. Cultivation Performance of T. subcordiformis

The growth dynamics of *T. subcordiformis* clearly depended on the quality of the culture medium, as confirmed by statistically significant differences between the experimental variants ($p \leq 0.05$). The highest yield was obtained in variant V2, where the final biomass concentration reached 1020 ± 108 mg VS/L, and the exponential phase lasted from day 2 to day 10 of cultivation (Figure 3a,b). The growth rate during this period (101.5 ± 15.2 mg VS/L·d) and the total biomass increase (826 ± 82 mg VS/L) indicate efficient utilisation of mixotrophic conditions (Table 5). The stable and prolonged exponential phase suggests that medium V2 provided a carbon-to-nitrogen-to-phosphorus ratio that supported photosynthetic and/or heterotrophic activity (mixotrophy), which is frequently emphasised in the literature as a key factor enhancing microalgal productivity [28]. According to Yang et al. [29], during active growth of microalgae, maximum biomass productivity is a combination of growth rate and the content of carbon reserves, which are generally inversely proportional. Therefore, a nutrient-rich medium promotes biomass formation, whereas nutrient limitation triggers intracellular storage of reserve products [30].

Variant V1 exhibited similar, though slightly lower, growth dynamics compared to V2, with a final biomass concentration of 970 ± 102 mg VS/L (Figure 3a). The exponential growth rate of 89.7 ± 14.5 mg VS/L·d was lower than in V2; however, this difference was not statistically significant ($p > 0.05$) (Table 5). The somewhat smaller biomass increase during the exponential phase indicates that the composition of medium V1 was less metabolically favourable, although it still supported relatively efficient population growth. This may have resulted from differences in the availability of key macronutrients, leading to earlier entry into the stationary phase—typical behaviour in environments with suboptimal C:N:P ratios [31]. Fernandes et al. [32] showed that microalgae respond to changes in nutrient ratios in two ways: they may maintain homeostasis by sustaining constant biomass composition and cellular functionality at the cost of growth rate, or restructure metabolic pathways and resource utilisation strategies to better adapt to new conditions.

According to Qian et al. [33], improper macronutrient ratios in the culture medium reduce microalgal biomass accumulation due to inhibition of photosynthesis, lowered oxidative stress resistance, and reduced metabolic activity. Similar conclusions were presented by Magyar et al. [34], who observed that increased nitrate concentrations stimulate chlorophyll formation and biomass growth, while elevated phosphate concentrations positively correlate with microalgal activity. They also reported that higher N:P ratios correspond to

higher chlorophyll concentrations. This indicates that both the C:N:P ratio and the absolute concentrations of nutrients in the medium directly influence microalgal growth rate and biomass yield [29,35].

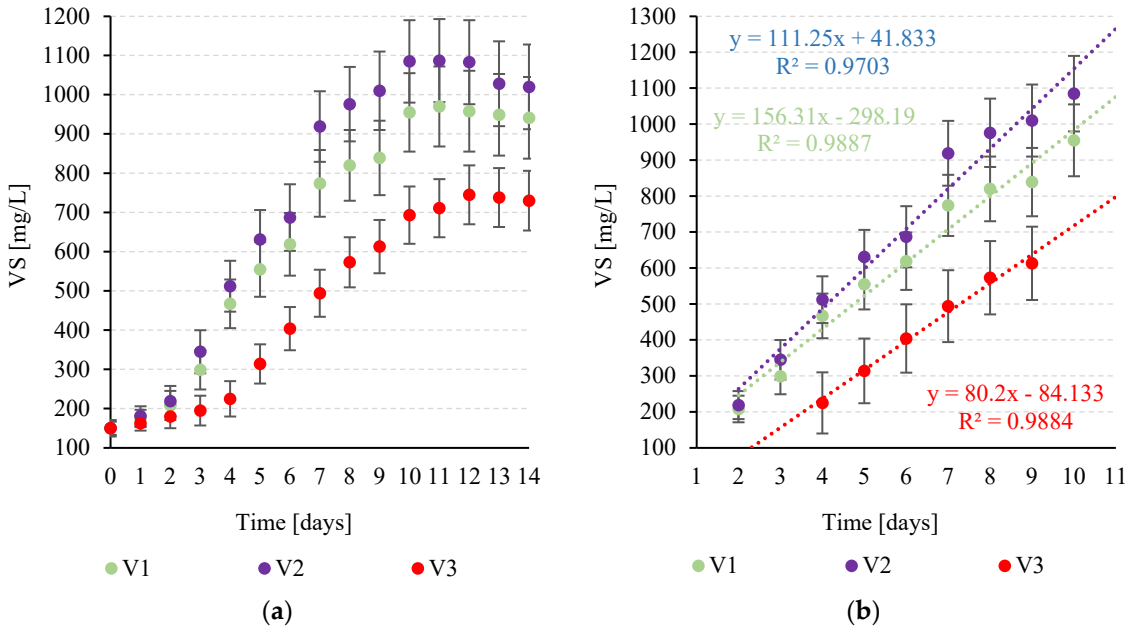


Figure 3. Growth curves of *T. subcordiformis* (**a**) and the progression of the exponential growth phase (**b**) according to the experimental variant.

Table 5. Indicators characterising the developmental phases of *T. subcordiformis* populations in the experimental cultivation variants.

Variant	Growth Phase	Duration [Days]	Total Increase [mg VS/L]	Growth Rate [mg VS/L·d]
V1	Lag	0–2	78 ± 36.3	15.2 ± 4.8
	Exponential	2–10	661 ± 79.0	89.7 ± 14.5
	Stationary	10–11	66 ± 102.7	5.2 ± 2.1
	Death	11–14	−6 ± 104.3	−3.5 ± 1.8
V2	Lag	0–2	109 ± 32.3	18.0 ± 5.0
	Exponential	2–10	826 ± 82.0	101.5 ± 15.2
	Stationary	10–12	2 ± 106.0	0.1 ± 0.3
	Death	12–14	−67 ± 107.7	−6.3 ± 2.5
V3	Lag	0–4	75 ± 18.0	32.0 ± 6.5
	Exponential	4–9	388 ± 47.0	77.6 ± 7.1
	Stationary	9–11	30 ± 71.7	3.1 ± 1.2
	Death	11–14	−23 ± 75.0	−6.8 ± 2.3

The greatest growth limitations were observed in variant V3, where the differences were statistically significant compared to V1 and V2 ($p \leq 0.05$). The lag phase lasted as long as four days, indicating slowed adaptation of cells to environmental conditions (Table 5). The exponential phase was shortened to the period between days 4 and 9 of cultivation, and the growth rate (77.6 ± 7.1 mg VS/L·d) was the lowest among all variants (Figure 3b). The total biomass increase reached 388 ± 57 mg VS/L, and the final biomass concentration

was 730 ± 76 mg VS/L, corresponding to a reduction in productivity of approximately 30–35% relative to V2 (Figure 3a).

These clearly reduced growth dynamics align with mechanisms of metabolic stress induced by the unfavourable properties of medium V3, which was characterised by the highest concentrations of TSS (1550 ± 450 mg/L) and lipids (80 ± 43 mg/L). Such an environment may generate several overlapping inhibitory effects. Under abiotic stress caused by contaminants present in wastewater, the balance between the production and suppression of reactive oxygen species (ROS) in algal cells is disrupted, leading to increased ROS levels [36]. Excessive ROS generation can damage microalgal cell components, including lipids, proteins, and the cell membrane [37]. This necessitates activation of protective systems and metabolic slowdown, reducing growth efficiency [38].

Similarly, the high content of suspended solids reduced light penetration and impaired effective photosynthesis, which in a mixotrophic strategy represents an additional factor limiting metabolic flexibility [39,40]. Excessive lipid concentrations may also destabilise cell membranes and increase ROS production, leading to oxidative stress that inhibits the activity of enzymes responsible for nitrogen and carbon metabolism [41,42]. This phenomenon is widely documented in microalgae exposed to high organic loading [40,43]. According to Lacroux et al. [30], heterotrophic growth of microalgae slows at low initial organic substrate concentrations, resulting in a greater contribution of autotrophic metabolism. This corresponds with the observed reduction in biomass increase as substrate concentration increases, since cells incorporate less external inorganic carbon. Furthermore, increased medium viscosity and elevated TSS may impede mass transfer and delay substrate diffusion, which explains the extended lag phase [36]. Under such conditions, microalgae shift to a metabolic dormancy strategy, reducing biosynthetic processes and delaying activation of mixotrophic pathways, consistent with the observed growth parameters [44].

To provide a reference framework for evaluating the efficiency of *T. subcordiformis* growth on the MFC anode effluent, the obtained results were compared with data reported for cultivation on defined synthetic/mineral media as well as on other alternative waste-derived media. Under control conditions, where a clean medium prepared from chemical reagents and deionized water is applied, biomass yields of this species are substantially higher than those achieved on real waste streams. For instance, Dudek et al. reported a final biomass concentration of 3410 ± 162 mgVS/L with a growth rate of 321 ± 21 mgVS/L·d for a control culture operated on a chemical medium [18]. Similarly, in the study by Dębsowski et al., the control variant (synthetic medium) enabled the attainment of a final biomass concentration of 2560 ± 301 mgVS/L [45].

Against this background, the results of the present manuscript indicate that the use of anode chamber effluent from an MFC fed with fruit and vegetable processing wastewater ensured stable, albeit markedly lower, biomass growth, ranging from 745 ± 75 mgVS/L (V3) to 1020 ± 108 mgVS/L (V2). In the study by Zieliński et al. [46], cultivation of *T. subcordiformis* on MFC effluent resulted in a final biomass concentration of approximately 1.1 gVS/L, whereas the control variant (clean mineral medium) achieved biomass yields of 2720 ± 199 mgVS/L. The observed reduction in productivity relative to synthetic controls is typical of systems in which the cultivation medium is a wastewater-derived stream or originates from bioelectrochemical processes. In the same study, higher technological performance was reported for soil-less agricultural wastewater, where the final microalgal concentration in a VT-PBR reached 3030 ± 183 mgVS/L [46]. Importantly, the key advantage of the strategy proposed in this work lies in the valorization of an effluent stream that would otherwise require further treatment/neutralisation prior to environmental discharge, while simultaneously generating functional biomass suitable for subsequent H_2 production.

Cultivation conditions based on the MFC anode effluent promote a shift of *T. subcordiformis* toward mixotrophic growth, as the medium contains both inorganic carbon as well as residual fractions of organic carbon (COD) and nutrients. This enables simultaneous CO_2 assimilation and uptake of organic compounds, resulting in redistribution of metabolic fluxes between biomass biosynthesis and carbon storage (carbohydrates/lipids) [47]. Differences in OLR/HRT (V1–V3) determined the quality of the anode effluent and the availability of readily assimilable carbon fractions, which may explain the observed changes in growth kinetics. In variants V1–V2, a moderate level of residual COD together with available nutrients supported intensive biosynthesis (higher μ and higher biomass concentration), whereas under the highest OLR (V3) part of the metabolic flux may have been redirected toward adaptive mechanisms and energetically costly stress responses, which is consistent with the observed growth deceleration [46]. The decrease in biomass productivity in V3 can also be interpreted as a consequence of physiological stress induced by the properties of the waste-derived medium. Elevated turbidity (TSS) and the presence of hydrophobic fractions (lipids) reduce light penetration and impair the performance of the photosynthetic apparatus, thereby promoting ROS generation and triggering antioxidant responses. Under such conditions, increased activity of antioxidant enzymes (e.g., SOD, catalase) and intensified lipid peroxidation (e.g., MDA) have been reported, leading to reduced growth rate, changes in chlorophyll content, and modifications in the biochemical composition of biomass [48]. This mechanism is particularly relevant in integrated bioenergy systems, as oxidative stress and redox imbalance may limit not only biomass accumulation but also the efficiency of photobiological H_2 production by affecting hydrogenase activity, its oxygen sensitivity, and the cellular redox state [49].

A literature review indicates that anaerobic digestate effluents can be effectively used as cultivation media for the growth of various microalgal species [50,51]. Scarponi et al. [52] reported that during the cultivation of *Chlorella vulgaris* on digestates derived from the anaerobic biodegradation of the organic fraction of municipal solid waste and activated sludge, biomass concentrations of 0.6–2.0 gVS/L were achieved. Comparable values were reported by Zuliani et al. [53], who obtained 2.00 gVS/L of *C. vulgaris* biomass and 1.75 gVS/L of *Scenedesmus obliquus* biomass using anaerobic digestate from the treatment of agricultural waste and sewage sludge. In other studies, biomass production of *C. vulgaris* on diluted digestate from the anaerobic treatment of municipal wastewater reached 0.6–3.01 gVS/L [54,55].

3.2. Nutrient Assimilation Efficiency in the Culture Medium

The results indicate that the quality of the culture medium played a key role not only in determining the growth dynamics of *T. subcordiformis* but also in the efficiency of assimilating major nutrients. Variants V1 and V2, characterised by elevated sugar concentrations and relatively low lipid content, promoted rapid development of microalgal populations under mixotrophic conditions. The achieved biomass concentrations—970 ± 102 mg VS/L in V1 and 1087 ± 106 mg VS/L in V2—combined with high growth rates in the logarithmic phase, respectively, 89.7 ± 14.5 and 101.5 ± 15.2 mg VS/L·d, indicate that the availability of easily accessible carbohydrates may significantly enhance biomass synthesis through synergistic utilisation of energy derived from both photosynthesis and heterotrophic sugar metabolism [56,57].

This phenomenon, widely described in the literature, is characteristic of microalgae engaged in mixotrophic growth, where an additional carbon source compensates for limitations associated with light intensity or micronutrient availability [58,59]. Nápoles-Armenta et al. [60] compared growth profiles of microalgae under autotrophic and heterotrophic conditions, observing that in mixotrophic cultivation, energy could be continuously pro-

duced by aerobic catabolism of organic compounds and by conversion of light energy into chemical energy via photosynthesis. This improvement enhanced nutrient transport and adsorption into cells, resulting in increased biomass production and higher growth rates compared to autotrophic cultures. According to Zhang et al. [56], intermediates of glycolysis may directly diffuse into chloroplasts and substitute for CO_2 bound by RuBisCO, serving as sources of carbon for organic carbon metabolism in the chloroplast.

High growth rates in V1 and V2 were also reflected in efficient nitrogen and phosphorus utilisation. The removal efficiencies of TN and NH_4-N remained similar, at 48–49%, confirming stable activity of enzymes responsible for the assimilation of inorganic nitrogen forms (Table 6). Final TN concentrations in both variants (111 ± 12 and 110 ± 13 mg/L) as well as NH_4-N (52 ± 6 and 56 ± 7 mg/L) show that nitrogen uptake rates were sufficiently high to sustain intensive biomass growth throughout the experiment. A similar pattern was observed for phosphorus. Removal efficiencies reached 62–63% for TP and 59–60% for PO_4-P, with final concentrations between 8.0–8.3 mg/L and 5.3–5.6 mg/L, respectively. These results indicate increased nutrient demand by actively growing cells during periods of high metabolic activity (Table 5). Literature on *Tetraselmis* species consistently emphasises their capacity for effective phosphorus biosorption and the formation of intracellular polyphosphate reserves, particularly in environments enriched in readily assimilable carbon [61]. Michels et al. [62] achieved 99% phosphorus removal during *Tetraselmis suecica* cultivation in fish-farm wastewater. Similarly, Goswami et al. [63] reported more than 90% phosphate removal within seven days of *T. suecica* growth. In contrast, Amit et al. [64] recorded lower efficiency, approximately 60.93%, during T. indica cultivation in domestic wastewater.

Table 6. Indicators characterising nutrient utilisation in the culture medium by *T. subcordiformis* biomass in the experimental variants.

Indicator	Unit	V1	V2	V3
Final biomass concentration	mg VS/L	970 ± 102	1087 ± 106	745 ± 75
VS linear growth phase	dni	2–10	2–10	4–9
VS growth rate in the logarithmic growth phase	mg VS/L·d	89.7 ± 14.5	101.5 ± 15.2	77.6 ± 7.1
TN utilisation rate for biomass growth	mg TN/g VS	31.4 ± 4.8	32.1 ± 5.1	28.7 ± 4.3
TN removal efficiency	%	48.7 ± 5.2	49.1 ± 5.4	42.3 ± 4.7
Final TN concentration	mg/L	111 ± 12	110 ± 13	130 ± 12
N-NH_4 utilisation rate for biomass growth	mg N-NH_4/g VS	14.5 ± 2.3	15.2 ± 2.5	12.8 ± 2.0
N-NH_4 removal efficiency	%	48.1 ± 5.1	49.0 ± 5.3	41.2 ± 4.5
Final N-NH_4 concentration	mg/L	52 ± 6	56 ± 7	76 ± 8
TP utilisation rate for biomass growth	mg TP/g VS	13.7 ± 2.0	14.2 ± 2.1	12.1 ± 1.7
TP removal efficiency	%	62.3 ± 6.2	63.1 ± 6.5	55.0 ± 5.0
Final TP concentration	mg/L	8 ± 1	8.3 ± 1.2	11.3 ± 1.5
P-PO_4 utilisation rate for biomass growth	mg P-PO_4/g VS	7.8 ± 1.2	8.1 ± 1.3	6.9 ± 1.1
P-PO_4 removal efficiency	%	59.0 ± 5.8	60.3 ± 6.0	52.0 ± 4.7
Final P-PO_4 concentration	mg/L	5.3 ± 0.7	5.6 ± 0.8	6.7 ± 0.9
COD utilisation rate for biomass growth	mg COD/g VS	210 ± 25	225 ± 28	180 ± 20
COD removal efficiency	%	43.5 ± 4.5	44.8 ± 5.0	36.7 ± 4.1

Table 6. *Cont.*

Indicator	Unit	V1	V2	V3
Final COD concentration	mg O_2/L	1190 ± 120	1 240 ± 135	2030 ± 160
TOC utilisation rate for biomass growth	mg TOC/g VS	180 ± 22	192 ± 24	158 ± 18
TOC removal efficiency	%	46.7 ± 5.0	48.0 ± 5.2	39.5 ± 4.3
Final TOC concentration	mg/L	96 ± 11	100 ± 12	123 ± 14

The average phosphorus content in algal cells is approximately 1%, and increases in its content indicate potential for enhanced phosphorus removal via biomass growth and synthesis of phosphorus-containing cellular constituents such as phospholipids and polyphosphate storage [65]. Microalgae may increase phosphorus uptake immediately after deficiency periods, as well as under excess conditions [66]. In response to phosphorus depletion, microalgae produce phosphatases with activities stimulated by low phosphate availability [67]. Cells generally accumulate polyphosphate when phosphorus is abundant in the environment [68]. Assimilation of inorganic phosphorus is controlled by active transporters whose kinetics depend on the acclimation state of cells, available energy for converting inorganic phosphorus into polyphosphate, and cellular phosphorus demand [69].

Higher microalgal biomass also contributes to nitrogen reduction in wastewater. According to Ge et al. [70], *Tetraselmis* species exhibit high potential for nitrogen removal, with ammonium being the preferred nitrogen substrate [71]. When ammonium is insufficient, microalgae assimilate nitrite and nitrate, which are enzymatically converted to ammonium by nitrate reductase [72].

Significant differences between the variants also appeared in the utilisation of organic carbon. In V1 and V2, stable COD reduction at 43.5–44.8% and TOC reduction at 46.7–48.0% were recorded, confirming that moderate carbon loading promotes a balance between autotrophy and heterotrophy and allows the maintenance of high metabolic activity (Table 6).

The most pronounced deviations were observed in variant V3, where the final biomass concentration reached only 745 ± 75 mg VS/L, while the growth rate decreased to 77.6 ± 7.1 mg VS/L·d. Despite greater initial nutrient availability, utilisation efficiencies were significantly lower, amounting to 42.3% for TN and 41.2% for N-NH_4, and for phosphorus, 55.0% (TP) and 52.0% (P-PO_4) (Table 6). This phenomenon aligns with the concept of substrate inhibition, which occurs under excessive availability of carbon-based organic compounds, particularly lipids [73,74]. The high lipid content in medium V3 may have led to disturbances in the stability, intensification of oxidative stress, and inhibition of enzyme activity responsible for nitrogen and carbon utilisation, consistent with reports on the effects of elevated organic loading on microalgal metabolism [75]. The final TOC and COD values in variant V3, at 123 ± 14 mg/L and 2030 ± 160 mg O_2/L respectively, indicate that in this variant, the mechanisms of degradation and assimilation of organic compounds were significantly weakened.

This trend is consistent with the bioelectrochemical characteristics of MFC operation, indicating that at the highest OLR a larger fraction of electrons was diverted to competing anaerobic pathways rather than being recovered as electrical current. The electrochemical parameters of an MFC represent useful indicators of anode-biofilm activity and the intensity of bioelectrochemical processes, which translate into the degree of pollutant bioconversion and the quality of the anode effluent subsequently used as a cultivation medium [76]. In the present study, changes in OLR and HRT resulted in significant differences in the electrical performance of the cell (Table 3). Increasing the OLR

from 1.0 to 2.0 g COD/L·d increased the average voltage from 313 ± 67 to 410 ± 85 mV and the current from 0.313 ± 0.067 to 0.410 ± 0.085 mA. At the same time, power density increased from 35 ± 5 to 60 ± 25 mW/m^2, and the average power rose from 0.098 ± 0.042 to 0.168 ± 0.070 mW. This indicates that V2 provided the most favourable conditions for anode respiration and extracellular electron transfer. This effect was consistent with the quality of the anode chamber effluent, which in variants V1–V2 was characterised by markedly lower COD (approximately 2100–2250 mg O_2/L) and clearly reduced suspended solids and lipid content (Table 2). At the highest loading, i.e., OLR = 3.0 g COD/L·d, relatively high voltage and power density were maintained; however, the average current decreased to 0.392 ± 0.107 mA and coulombic efficiency dropped to 11 ± 5% (Table 3). This phenomenon indicates a reduction in the electrochemical efficiency of the bioanode and a greater contribution of processes competing with electron transfer to the anode [77]. Concurrently, variant V3 showed deterioration in effluent quality: residual COD increased to 3200 ± 1460 mg O_2/L, suspended solids reached 1550 ± 450 mg/L, and lipid content increased to 80 ± 43 mg/L (Table 2).

The decrease in coulombic efficiency and current observed in variant V3, despite the maintenance of relatively high voltage and power density, indicates a shift in the electron balance toward pathways competing with anode respiration. Under high organic loading (OLR = 3.0 g COD/L·d) and shortened HRT, the contribution of hydrolysis and fermentation increases and intermediate products (e.g., VFAs) tend to accumulate, which promotes electron consumption for metabolite reduction and heterotrophic biomass growth rather than transfer to the anode, thereby reducing CE [78]. Concurrently, competitive pressure from non-electroactive microorganisms, including methanogens, increases, resulting in electron "loss" to CH_4 formation and a further decline in charge recovery as electrical current [79]. Moreover, high OLR in fruit and vegetable processing wastewater is typically associated with elevated TSS and a higher share of hydrophobic fractions (lipids), which may limit mass transfer to the biofilm, impair biofilm–electrode contact, and slow extracellular electron transfer (EET) through both direct (cytochromes/conductive nanostructures) and indirect (redox mediators) mechanisms. Additional limiting factors may include local biofilm acidification and increased internal resistance, which intensify kinetic and transport constraints [80]. These mechanisms are consistent with the observed deterioration of effluent quality in V3 (higher residual COD, TSS, and lipid content), suggesting a lower degree of electrochemical bioconversion and a higher proportion of residual fractions in the effluent medium [81].

The results suggest that not only the quantity of available substrates determines the growth performance of *T. subcordiformis* and thus the efficiency of nutrient assimilation processes. Variants rich in sugars promoted intensive biomass growth and high nitrogen and phosphorus assimilation efficiency, whereas medium with increased lipid content limited the metabolic rate, leading to a clear reduction in both biomass accumulation and organic substrate removal. The observed relationships are consistent with current knowledge in microalgal biology and environmental biotechnology and provide important insights for optimising cultivation conditions in systems aimed at biomass productivity or nutrient removal [82,83].

In natural and exponentially growing phytoplankton populations, the observed Redfield ratio C:N:P is 106:16:1, reflecting fundamental cellular properties [84,85]. Nevertheless, elemental ratios in algal cells are not constant and may undergo dynamic changes reflecting variations in the biochemical composition of the culture medium [31]. As demonstrated in studies by various authors, the N:P ratio in algal cells changes with nutrient availability, and a generally positive correlation is observed between the cellular N:P ratio and the supply ratio of these elements in the medium [84,86]. Conversely, a high C:N ratio results

in a decrease in cellular protein concentration, a reduction in chlorophyll a content, and contributes to the accumulation of storage compounds [31,87].

It has been demonstrated that optimisation of ammonia concentration is a key factor affecting microalgal growth performance and their ability to remove N and P from anaerobic digestate [52]. Jhouhanggir et al. [51] showed that during the cultivation of *C. vulgaris* on anaerobic digestate at a C/N ratio of 6.47 ± 1.15, the removal efficiencies of COD and ammonium nitrogen reached 89.02 ± 0.84% and 89.45 ± 1.29% (NH_4^+-N), respectively. Similarly, Ledda et al. [88] reported effective elimination of organic compounds and nitrogen, achieving 61–73% COD removal and 95–98% NH_4^+-N removal during *C. vulgaris* cultivation on anaerobic digestate. In turn, cultivation of *Scenedesmus dimorphus* on anaerobic digestate resulted in high removal efficiencies of organic matter, nitrogen, and phosphorus of 65–72% COD, 63–100% N, and 78–82% P, respectively, as well as complete ammonia elimination [89].

3.3. Characteristics and Properties of T. subcordiformis Biomass

The composition of *T. subcordiformis* biomass varied according to cultivation conditions, reflecting both the cells' capacity to accumulate organic matter and their adaptive responses to changing environmental parameters. In variant V1, the VS content was 86.2 ± 2.8% of dry mass, while in V2 it reached 88.5 ± 3.1%, with no statistically significant difference ($p > 0.05$) (Table 7). A similar pattern was observed for organic carbon content, which in V1 was 505.3 ± 21.7 mg/g VS, and in V2 increased to 530.6 ± 23.5 mg/g VS ($p > 0.05$). The absence of statistical differences indicates that both conditions enabled cells to maintain comparable rates of carbon assimilation. This phenomenon is often observed in microalgal cultures developing under reduced light availability or nutrient limitation. Under such conditions, cells reduce their division rate but continue to accumulate organic matter to sustain basic physiological processes [90].

Table 7. Biochemical composition of *T. subcordiformis* biomass in the cultivation variants.

Parameter	Unit	V1	V2	V3
Volatile solids (VS)	% TS	86.2 ± 2.8	88.5 ± 3.1	85.3 ± 3.6
Mineral solids (MS)	% TS	13.8 ± 2.8	11.5 ± 3.1	14.7 ± 3.6
Total carbon (TC)	mg/g VS	540.7 ± 26.4	565.3 ± 28.9	528.4 ± 25.7
Total organic carbon (TOC)	mg/g VS	505.3 ± 21.7	530.6 ± 23.5	498.1 ± 22.4
TN	mg/g VS	48.2 ± 3.4	50.1 ± 3.7	46.5 ± 3.9
C/N ratio	—	10.5 ± 0.7	10.6 ± 0.8	10.7 ± 0.7
TP	mg/g VS	11.3 ± 0.9	12.0 ± 1.1	10.8 ± 0.9
pH of the biomass	—	7.18 ± 0.19	7.12 ± 0.17	7.05 ± 0.21
Protein	mg/g VS	370.4 ± 28.5	402.7 ± 31.2	355.1 ± 29.8
Soluble sugars	mg/g VS	135.6 ± 16.4	142.3 ± 18.2	130.4 ± 15.7
Lipids	mg/g VS	72.5 ± 11.8	78.3 ± 12.5	80.7 ± 13.6

Protein and carbohydrate fractions were also similar between V1 and V2. Protein content was 370.4 ± 28.5 mg/g VS in V1 and 402.7 ± 31.2 mg/g VS in V2 ($p > 0.05$), while carbohydrate content was 135.6 ± 16.4 mg/g VS in V1 and 142.3 ± 18.2 mg/g VS in V2 ($p > 0.05$). However, variant V2 was characterised by a higher phosphorus content, amounting to 12.0 ± 1.1 mg/g VS, whereas in V1 the phosphorus level was 11.3 ± 0.9 mg/g VS ($p > 0.05$) (Table 7). Although the difference was not statistically significant, the slightly greater accumulation of phosphorus may have enhanced the cells' capacity for ATP and

nucleic acid synthesis, corresponding with the slightly higher protein and carbohydrate content observed in V2. Microalgae often respond in this way when phosphorus availability is sufficient but the growth rate remains low, with part of the surplus phosphate stored within cellular structures [68].

A distinct biochemical profile of the microalgae was identified in variant V3. The content of volatile substances decreased to 85.3 ± 3.6% of dry mass and was significantly lower than in V2 ($p \leq 0.05$). Similarly, the organic carbon content declined to 498.1 ± 22.4 mg/g VS, also with statistical significance ($p \leq 0.05$) (Table 7). Such a reduction in the organic fraction typically indicates a limited ability of cells to accumulate carbon, which may result from both deteriorated light conditions and disturbances in nutrient transport in a more heavily loaded medium [91]. This mechanism is well described for microalgae that, under environmental stress, reduce photosynthetic activity and are unable to maintain high organic content per unit mass [92].

An even more pronounced signal of reduced biosynthetic activity appeared in the protein and carbohydrate analyses. In variant V3, protein content declined to 355.1 ± 29.8 mg/g VS, and carbohydrate content to 130.4 ± 15.7 mg/g VS (Table 7). These changes were statistically significant compared with V2 ($p \leq 0.05$). The reduction in these fractions indicates that the cells encountered conditions that disrupted the synthesis of metabolites requiring substantial energy input. The literature shows that microalgae, under low phosphorus availability or when photosynthesis is impaired, first reduce protein synthesis [66,70], which is precisely reflected in the results of variant V3. This is associated with inhibition of phosphorus-dependent processes (ATP and nucleotide synthesis) and with adaptive transcriptomic reprogramming, in which cells reduce protein synthesis and the biogenesis of the photosynthetic apparatus, while excess carbon is redirected towards lipid or polysaccharide accumulation, resulting in a decline in total biomass productivity [29]. Studies by Plouviez et al. [93] confirm that transcriptomic and proteomic responses of genes and proteins associated with phosphorus availability are synchronised, and regulation of the C:N:P ratio may enhance the ability of algal cells to produce high concentrations of carbohydrates, proteins, or lipids [94].

The biomass obtained in V3 was characterised by a phosphorus content of 10.8 ± 0.9 mg/g VS, significantly lower than in V2 ($p \leq 0.05$). This may indicate disturbances in phosphate transport or incorporation into cellular structures. Since phosphorus, as previously mentioned, is essential for ATP synthesis, nucleotide formation, and membrane phospholipid production, its reduced availability may directly inhibit the formation of proteins and carbohydrates, which is consistent with the results obtained. Under stress conditions, microalgae often compensate for this deficit by reducing growth and entering a state of metabolic conservation, including phosphorus redistribution, storage as polyphosphates, lipid accumulation, reduced photosynthetic rate, and lowered biomass productivity [95].

In V3, an increase in lipid content was also observed, reaching 80.7 ± 13.6 mg/g VS. This value was higher than in V2 (78.3 ± 12.5 mg/g VS) and V1 (72.5 ± 11.8 mg/g VS), although the differences were not statistically significant ($p > 0.05$) (Table 6). It is likely that microalgae increased lipid production under conditions of limited nitrogenous metabolite synthesis, which is widely recognised as an indicator of cellular stress [96]. This phenomenon is characteristic of cultures with low growth rates, which first reduce protein metabolism [66]. A review of the literature indicates that phosphorus concentration and light intensity have a decisive influence on protein synthesis in algal cells, with higher phosphorus levels generally increasing protein content, whereas low light favours protein accumulation at the expense of lipids and carbohydrates [97].

3.4. Biohydrogen Production

The total H_2 production in V1 and V2 was similar, with no significant differences ($p > 0.05$), amounting to 182.3 ± 23.1 mL and 184.7 ± 25.0 mL, respectively (Figure 4a,b). Comparable values were also obtained for the kinetic parameters: the reaction rate constant was 0.0435 ± 0.0051 1/h in V1 and 0.0441 ± 0.0054 1/h in V2 (Table 8). The hydrogen production rate reached 8.74 ± 1.11 mL/h and 8.85 ± 1.19 mL/h, respectively ($p > 0.05$). The unit hydrogen production in V1 was 193.7 ± 32.6 mL H_2/g VS, while in V2 it was 181.1 ± 31.1 mL H_2/g VS (Figure 4d). These high and comparable values indicate a very good metabolic condition of individual cells, which, despite challenging environmental conditions and limited biomass growth rates, maintained high efficiency in converting light energy into H_2. The literature confirms that stability of the specific activity of hydrogenase is characteristic of cultures functioning under moderate, but not extreme, stress conditions [98].

Table 8. Basic kinetic parameters of H_2 production by *T. subcordiformis* and biogas composition.

Parameter	Unit	V1	V2	V3
Total biomass	mg VS	941 ± 104	1020 ± 108	730 ± 76
Total H_2 production	mL	182.3 ± 23.1	184.7 ± 25.0	112.0 ± 14.8
H_2 production rate constant (k)	1/h	0.0435 ± 0.0051	0.0441 ± 0.0054	0.0348 ± 0.0045
H_2 production rate (r)	mL/h	8.74 ± 1.11	8.85 ± 1.19	5.35 ± 0.70
Specific H_2 production (unique H_2)	mL/g VS	193.7 ± 32.6	181.1 ± 31.1	153.4 ± 25.8
Biogas composition—H_2	%	58.2 ± 4.5	58.7 ± 4.6	58.0 ± 4.4
Biogas composition—CO_2	%	35.6 ± 3.8	35.3 ± 3.7	35.9 ± 3.9
Biogas composition—O_2	%	6.2 ± 1.2	6.0 ± 1.3	6.1 ± 1.1

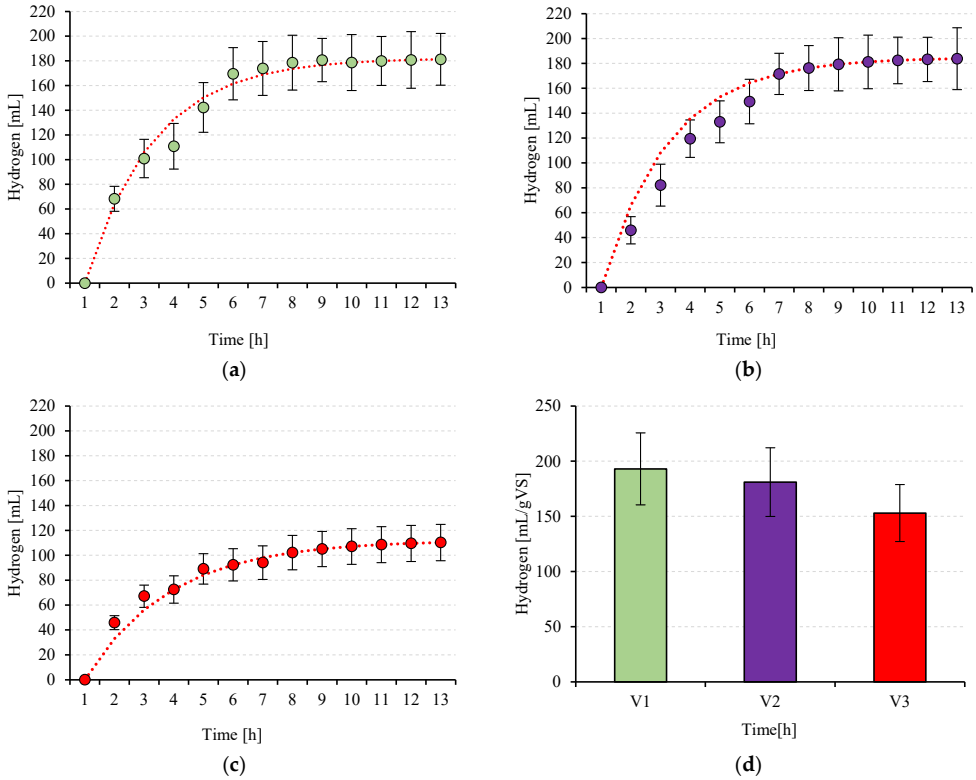


Figure 4. Hydrogen production by *T. subcordiformis* in V1 (**a**), V2 (**b**), V3 (**c**), and comparison of final gas yields (**d**).

Hydrogenase is highly sensitive to oxygen concentration in the environment; therefore, under aerobic conditions or when excess O_2 is produced during photosynthesis, it becomes deactivated [99]. When the environment becomes too stressful (e.g., severe nutrient deficiency, intense oxidative stress, degradation of the photosynthetic apparatus), cells often lose photosynthetic activity, may have damaged photosystems, reduced efficiency of electron transfer, and consequently exhibit markedly lower or unstable H_2 production [100]. Conversely, properly controlled environmental conditions strongly promote long-term and stable hydrogenase activity, and thus high efficiency of photobiological H_2 production. This includes maintaining oxygen balance to limit photogenic O_2 accumulation, which deactivates [FeFe]-hydrogenase, as well as ensuring a continuous supply of electrons generated in photosynthetic processes [100]. At the same time, creating functional protective zones around the enzyme is essential—local microenvironments with reduced oxygen content formed, for example, inside cell aggregates, biofilms, immobilised systems, or environments with controlled, slightly acidifying or buffered pH [101,102]. Such conditions limit O_2 diffusion into cells and stabilise redox parameters, while maintaining hydrogenase activity even when photosynthetic oxygen evolution still occurs [103]. As a result, these complex but stable microenvironments allow long-lasting enzyme functionality and efficient electron flow into the H_2 production pathway, leading to markedly higher and more stable photobiological hydrogen yields.

The presence of oxygen (ca. 6%) in the headspace during the hydrogen production stage requires clarification, as O_2 is a strong inhibitor of hydrogenase and its occurrence may limit H_2 yields. Despite applying a medium deoxygenation procedure, residual biological O_2 production may have occurred. The *T. subcordiformis* biomass was concentrated and subsequently transferred to sulphur (S)-depleted medium; however, S limitation does not result in an immediate shutdown of photosystem II (PSII). During the initial adaptation phase, cells may retain partial photosynthetic activity due to the existing photosynthetic apparatus and intracellular sulphur reserves [104]. Consequently, despite a 30 h dark phase, the application of a 90 h light phase could have promoted limited O_2 evolution. This is consistent with the S-deprivation mechanism used to induce H_2 production, in which the transition from photosynthetic conditions to full hydrogenase activation occurs gradually [104]. Importantly, the O_2 fraction measured in the headspace does not directly reflect conditions in the liquid phase. Due to limited diffusion and rapid oxygen consumption within the biomass suspension, microanoxic conditions conducive to hydrogenase activity could have been maintained in the medium despite detectable O_2 in the headspace.

The biomass amount in V3 reached only 730 ± 76 mg VS, representing a significant decrease compared with V1 and V2 ($p \leq 0.05$). Limited biomass means fewer cells capable of photosynthesis and biophotolysis. For this reason, the total H_2 production in V3 was significantly lower than in V1 and V2, amounting to 112.0 ± 14.8 mL (Figure 4c). The hydrogen production rate in V3 reached 5.35 ± 0.70 mL/h and was significantly lower than the values observed in V1 and V2 ($p \leq 0.05$), indicating a slowdown in electron flow through the photosynthetic chain and reduced hydrogenase activity at the level of the entire cell population. Importantly, reduced total H_2 production did not indicate a loss of potential for its generation. The unit hydrogen production in V3 reached 153.4 ± 25.8 mL/g VS, which, although lower than in V1 and V2, remained high, especially considering the significantly lower biomass amount. This result indicates that the population in V3 was less numerous but metabolically active, and the cells that survived under these conditions retained substantial photobiological H_2 production capacity. Such a profile is characteristic of microalgae functioning under moderate, selective stress: weaker cells are eliminated, while the population is maintained by units exhibiting higher enzymatic activity [105]. The proportions of gases remained within stable ranges: hydrogen 58.0–58.7%, carbon dioxide

approximately 35–36%, and oxygen around 6%, with no significant differences between variants ($p > 0.05$), indicating a stable biogas composition. The observed differences occurred only at the process scale, depending on the amount of biomass and reaction kinetics, not on the mechanism of biophotolysis itself.

Other microalgal and cyanobacterial species are also capable of coupling photosynthesis with biohydrogen production due to the presence of enzymes such as hydrogenases or nitrogenases [106]. Using *C. vulgaris* strains, photobiological H_2 production of 12 mL H_2/L·h has been achieved [107]. In other studies, *C. vulgaris* cells were maintained under alternating illumination in light/dark cycles, resulting in a maximum H_2 production rate of 34.8 mL/L·h [108]. Moreover, the application of violet light for cultivation of *C. vulgaris* and *S. obliquus* yielded hydrogen productivities of 204.8 mL/L·d and 39.18 mL/L·d, respectively [109].

Literature indicates that the amount of microalgal biomass directly affects total hydrogen production, as the number of active cells determines the available enzymatic centres responsible for generating H_2 [110,111]. Moderate stress conditions generally do not alter the metabolic pathways leading to H_2 generation; however, they may modulate the intensity of these pathways, increasing or decreasing their efficiency. This results only in quantitative differences in H_2 production, not in changes to the mechanism of its formation [112]. Furthermore, optimal lighting conditions increase H_2 production rates by suppressing photosynthetic oxygen evolution [113]. According to Arimbrathodi et al. [114], low microalgal cell density in the cultivation system regulates the amount of light passing through microalgal cells and effectively reduces dissolved oxygen uptake by the culture. In contrast, high cell density may lead to carbohydrate accumulation and inhibit the cell growth rate. Therefore, to achieve high H_2 production, the active growth phase of microalgae and appropriate cell density in the culture must be maintained [115].

4. Conclusions

The results indicate that the growth of *T. subcordiformis* and the ability of these microalgae to produce hydrogen were most effective in cultivation media with lower lipid content, moderate levels of organic compounds, and limited suspended solids. Under these conditions, the highest biomass concentrations, ranging from 970 to 1020 mg VS/L, were achieved, along with the greatest nutrient assimilation efficiency, particularly for nitrogen (approximately 49%) and phosphorus (62–63%). The microalgae also maintained a stable biomass composition, with a predominance of protein and lipid fractions, which may have supported higher photosynthetic and enzymatic activity. The cultivation medium parameters and relatively high biomass productivity directly translated into the highest total (182–185 mL) and unit hydrogen production yields (181–194 mL/g VS).

Conversely, media containing higher concentrations of lipids, TSS, and organic loading significantly limited biomass accumulation to 745 ± 75 mg VS/L, led to reduced nitrogen (approximately 42%) and phosphorus (approximately 55%) assimilation, and shifted the biomass composition towards an increased lipid fraction, a typical indicator of metabolic stress and decreased activity of nutrient transporters. As a result, total H_2 production decreased to 112.0 ± 14.8 mL, although unit production remained high at 153 ± 25 mL/g VS, suggesting that the cells surviving under more challenging conditions retained substantial enzymatic potential, but their number was insufficient to achieve higher total production.

The stable biogas composition under all tested conditions (H_2 58–59%, CO_2 35–36%, O_2 approximately 6%) confirms that differences in overall process efficiency were primarily driven by biomass quantity and quality as well as nutrient assimilation efficiency, rather than changes in photobiolysis mechanisms. The findings highlight that in bioenergy systems utilising biodegradable waste, controlling the quality of the cultivation medium is

crucial for increasing total biohydrogen production, mainly by supporting efficient growth of *T. subcordiformis* biomass.

The key contribution of this work is the demonstration of an alternative MFC–microalgae integration model, in which the fuel cell is not considered a system aimed at maximising electrical energy recovery, but rather a module generating an effluent stream that requires further neutralisation and can subsequently be valorized as a resource. The use of the marine microalga *T. subcordiformis* is of high practical relevance, as its salinity requirements limit conventional applications in MFC biocathodes, while enhancing the potential for valorization of anode effluents toward biomass production and a clean energy carrier. The obtained results confirm the feasibility of integrating wastewater treatment and resource recovery (carbon and nutrients) with biomass and hydrogen production within the circular economy framework, while indicating that a key implementation prerequisite is controlling the quality of the anode effluent (particularly TSS and lipids) through appropriate selection of OLR/HRT.

Author Contributions: Conceptualization, M.Z. and M.D.; methodology M.Z. and M.D.; validation, M.K.; formal analysis, M.D.; investigation, M.Z., M.K., P.R., J.K. and M.D.; resources, M.Z., M.K., P.R.,, J.K. and M.D.; data curation, M.Z., M.K., P.R., J.K. and M.D.; supervision, M.D.; writing—original draft preparation, M.K. and M.D.; writing—review and editing, M.Z., M.K., P.R., J.K. and M.D.; visualisation, M.K. and M.D.; funding acquisition, M.Z. All authors have read and agreed to the published version of the manuscript.

Funding: This work was financed by the Polish National Science Center (Grant Number: 2021/41/B/NZ9/02225).

Institutional Review Board Statement: Not applicable.

Data Availability Statement: The original contributions presented in this study are included in the article.

Conflicts of Interest: The authors declare no conflicts of interest.

References

1. Sułek, A.; Borowski, P.F. Business Models on the Energy Market in the Era of a Low-Emission Economy. *Energies* **2024**, *17*, 3235. [CrossRef]
2. Saini, R.K.; Saini, D.K.; Verma, P.; Thakur, R.; Gandotra, N.; Kumar, R.; Sharma, B.B.; Verma, A. Climate Change and Energy Transition–a Critical Review. *Int. J. Green. Energy* **2025**, *23*, 1–26. [CrossRef]
3. Dakal, T.C.; Singh, N.; Kaur, A.; Kaur Dhillon, P.; Bhatankar, J.; Meena, R.; Sharma, R.K.; Gadi, B.R.; Sahu, B.S.; Patel, A.; et al. New Horizons in Microbial Fuel Cell Technology: Applications, Challenges, and Prospects. *Biotechnol. Biofuels Bioprod.* **2025**, *18*, 79. [CrossRef] [PubMed]
4. Greenman, J.; Gajda, I.; Ieropoulos, I. Microbial Fuel Cells (MFC) and Microalgae; Photo Microbial Fuel Cell (PMFC) as Complete Recycling Machines. *Sustain. Energy Fuels* **2019**, *3*, 2546–2560. [CrossRef]
5. Mekuto, L.; Olowolafe, A.V.; Huberts, R.; Dyantyi, N.; Pandit, S.; Nomngongo, P. Microalgae as a Biocathode and Feedstock in Anode Chamber for a Self-Sustainable Microbial Fuel Cell Technology: A Review. *S. Afr. J. Chem. Eng.* **2020**, *31*, 7–16. [CrossRef]
6. Anandapadmanaban, B.H.; Liu, S.-H.; Lin, C.-W. Prospects of Microalgae in the Cathode Chamber of Microbial Fuel Cells: From Sequestration to Bioproduct Production. *Biomass Bioenergy* **2025**, *194*, 107616. [CrossRef]
7. Bolognesi, S.; Cecconet, D.; Callegari, A.; Capodaglio, A.G. Combined Microalgal Photobioreactor/Microbial Fuel Cell System: Performance Analysis Under Different Process Conditions. *Environ. Res.* **2021**, *192*, 110263. [CrossRef]
8. Salim, H.; Al Farraji, A.; Khadim, H.J. A Review on Microbial Fuel Cell–Photobioreactor (MFC-PBR) Systems: Wastewater Treatment, Bioenergy Recovery, and CO_2 Sequestration. *Int. J. Des. Nat. Ecodyn.* **2025**, *20*, 537–546. [CrossRef]
9. Mansoor, B.; Ashraf, S.; Rehman, U.; Ullah, Z.; Sheikh, Z. Integration of Microalgae–Microbial Fuel Cell with Microbial Electrolysis Cell for Wastewater Treatment and Energy Production. *Environ. Sci. Proc.* **2023**, *25*, 72. [CrossRef]
10. Ahirwar, A.; Khan, M.J.; Khandelwal, P.; Singh, G.; Harish; Vinayak, V.; Ghangrekar, M.M. Bioelectromics of a Photosynthetic Microalgae-Assisted Microbial Fuel Cell for Wastewater Treatment and Value-Added Production. *Sci. Rep.* **2025**, *15*, 30196. [CrossRef]

11. Logan, B.E.; Hamelers, B.; Rozendal, R.; Schröder, U.; Keller, J.; Freguia, S.; Aelterman, P.; Verstraete, W.; Rabaey, K. Microbial Fuel Cells: Methodology and Technology. *Environ. Sci. Technol.* **2006**, *40*, 5181–5192. [CrossRef] [PubMed]
12. Tay, Z.H.; Ng, F.L.; Ling, T.C.; Iwamoto, M.; Phang, S.M. The Use of Marine Microalgae in Microbial Fuel Cells, Photosynthetic Microbial Fuel Cells and Biophotovoltaic Platforms for Bioelectricity Generation. *3 Biotech.* **2022**, *12*, 148. [CrossRef] [PubMed]
13. Amalapridman, V.; Ofori, P.A.; Abbey, L. Valorization of Algal Biomass to Biofuel: A Review. *Biomass* **2025**, *5*, 26. [CrossRef]
14. Hasan, M.M.; Mofijur, M.; Uddin, M.N.; Kabir, Z.; Badruddin, I.A.; Khan, T.Y. Insights into anaerobic digestion of microalgal biomass for enhanced energy recovery. *Front. Energy Res.* **2024**, *12*, 1355686. [CrossRef]
15. Hawrot-Paw, M.; Drzewicka, W. Application of Rapeseed Oil Cake from Biodiesel Production in Methane Co-Digestion with Microalgal Biomass. *Materials* **2025**, *18*, 4542. [CrossRef]
16. Lucia, U.; Grisolia, G. Preliminary Considerations on the Co-Production of Biomethane and Ammonia from Algae and Bacteria. *Inventions* **2025**, *10*, 47. [CrossRef]
17. Santos-Ballardo, D.U.; Font-Segura, X.; Ferrer, A.S.; Barrena, R.; Rossi, S.; Valdez-Ortiz, A. Valorisation of Biodiesel Production Wastes: Anaerobic Digestion of Residual *Tetraselmis Suecica* Biomass and Co-Digestion with Glycerol. *Waste Manag. Res.* **2015**, *33*, 250–257. [CrossRef]
18. Dudek, M.; Dębowski, M.; Kazimierowicz, J.; Zieliński, M.; Quattrocelli, P.; Nowicka, A. The Cultivation of Biohydrogen-Producing *Tetraselmis Subcordiformis* Microalgae as the Third Stage of Dairy Wastewater Aerobic Treatment System. *Sustainability* **2022**, *14*, 12085. [CrossRef]
19. Dębowski, M.; Dudek, M.; Kazimierowicz, J.; Quattrocelli, P.; Rusanowska, P.; Barczak, Ł.; Nowicka, A.; Zieliński, M. Analysis of Multi-Biofuel Production During Cultivation of the Green Microalga *Tetraselmis Subscordiformis*. *Energies* **2024**, *17*, 3670. [CrossRef]
20. Yahampath Arachchige Don, C.D.Y.; Babel, S. Circulation of Anodic Effluent to the Cathode Chamber for Subsequent Treatment of Wastewater in Photosynthetic Microbial Fuel Cell with Generation of Bioelectricity and Algal Biomass. *Chemosphere* **2021**, *278*, 130455. [CrossRef]
21. Garcia-Peña, E.I.; Parameswaran, P.; Kang, D.W.; Canul-Chan, M.; Krajmalnik-Brown, R. Anaerobic Digestion and Co-Digestion Processes of Vegetable and Fruit Residues: Process and Microbial Ecology. *Bioresour. Technol.* **2011**, *102*, 9447–9455. [CrossRef]
22. Morales-Amaral, M.M.; Gómez-Serrano, C.; Acién, F.G.; Fernández-Sevilla, J.M.; Molina-Grima, E. Production of Microalgae Using Centrate from Anaerobic Digestion as the Nutrient Source. *Algal Res.* **2015**, *9*, 297–305. [CrossRef]
23. Psachoulia, P.; Schortsianiti, S.N.; Lortou, U.; Gkelis, S.; Chatzidoukas, C.; Samaras, P. Assessment of Nutrients Recovery Capacity and Biomass Growth of Four Microalgae Species in Anaerobic Digestion Effluent. *Water* **2022**, *14*, 221. [CrossRef]
24. Erkelens, M.; Ward, A.J.; Ball, A.S.; Lewis, D.M. Microalgae Digestate Effluent as a Growth Medium for Tetraselmis sp. in the Production of Biofuels. *Bioresour. Technol.* **2014**, *167*, 81–86. [CrossRef] [PubMed]
25. Available online: https://sagdb.uni-goettingen.de/culture_media/08%20Porphyridium%20Medium.pdf (accessed on 1 December 2025).
26. Dębowski, M.; Dudek, M.; Nowicka, A.; Quattrocelli, P.; Kazimierowicz, J.; Zieliński, M. Suitability of pre-digested dairy effluent for mixotrophic cultivation of the hydrogen-producing microalgae *Tetraselmis subcordiformis*. *Environ. Technol.* **2024**, *45*, 471–482. [CrossRef] [PubMed]
27. Aiba, S.; Ogawa, T. Assessment of Growth Yield of a Blue--green Alga, Spirulina platensis, in Axenic and Continuous Culture. *J. Gen. Microbiol.* **1977**, *102*, 179–182. [CrossRef]
28. Smith, R.T.; Bangert, K.; Wilkinson, S.J.; Gilmour, D.J. Synergistic Carbon Metabolism in a Fast-Growing Mixotrophic Freshwater Microalgal Species *Micractinium inermum*. *Biomass Bioenergy* **2015**, *82*, 73–86. [CrossRef]
29. Yang, F.; Xiang, W.; Li, T.; Long, L. Transcriptome Analysis for Phosphorus Starvation-Induced Lipid Accumulation in *Scenedesmus* sp. *Sci. Rep.* **2018**, *8*, 16420. [CrossRef]
30. Lacroux, J.; Seira, J.; Trably, E.; Bernet, N.; Steyer, J.P.; van Lis, R. Mixotrophic Growth of *Chlorella sorokiniana* on Acetate and Butyrate: Interplay Between Substrate, C:N Ratio and pH. *Front. Microbiol.* **2021**, *12*, 703614. [CrossRef]
31. Gao, B.; Liu, J.; Zhang, C.; Van de Waal, D.B. Biological Stoichiometry of Oleaginous Microalgal Lipid Synthesis: The Role of N:P Supply Ratios and Growth Rate on Microalgal Elemental and Biochemical Composition. *Algal Res.* **2018**, *32*, 353–361. [CrossRef]
32. Fernandes, T.; Fernandes, I.; Andrade, C.A.P.; Cordeiro, N. Assessing the Impact of Sulfur Concentrations on Growth and Biochemical Composition of Three Marine Microalgae. *J. Appl. Phycol.* **2020**, *32*, 967–975. [CrossRef]
33. Qian, W.; Yang, Y.; Chou, S.; Ge, S.; Li, P.; Wang, X.; Zhuang, L.-L.; Zhang, J. Effect of N/P Ratio on Attached Microalgae Growth and the Differentiated Metabolism Along the Depth of Biofilm. *Environ. Res.* **2024**, *240*, 117428. [CrossRef] [PubMed]
34. Magyar, T.; Németh, B.; Tamás, J.; Nagy, P.T. Improvement of N and P Ratio for Enhanced Biomass Productivity and Sustainable Cultivation of *Chlorella vulgaris* Microalgae. *Heliyon* **2024**, *10*, e23238. [CrossRef] [PubMed]
35. Faruque, M.O.; Ilyas, M.; Hossain, M.M.; Razzak, S.A. Influence of Nitrogen to Phosphorus Ratio and CO_2 Concentration on Lipid Accumulation of *Scenedesmus dimorphus* for Bioenergy Production and CO_2 Biofixation. *Chem. Asian J.* **2020**, *15*, 4307–4320. [CrossRef] [PubMed]

36. Ugya, A.Y.; Chen, H.; Wang, Q. Microalgae Biofilm System as an Efficient Tool for Wastewater Remediation and Potential Bioresources for Pharmaceutical Product Production: An Overview. *Int. J. Phytoremediation* **2024**, *26*, 131–142. [CrossRef]
37. Rezayian, M.; Niknam, V.; Ebrahimzadeh, H. Oxidative Damage and Antioxidative System in Algae. *Toxicol. Rep.* **2019**, *6*, 1309–1313. [CrossRef]
38. Milrad, Y.; Mosebach, L.; Buchert, F. Regulation of Microalgal Photosynthetic Electron Transfer. *Plants* **2024**, *13*, 2103. [CrossRef]
39. Jung, S.H.; McHardy, C.; Rauh, C.; Jahn, A.; Luzi, G.; Delgado, A.; Buchholz, R.; Lindenbergar, C. A New Approach for Calculating Microalgae Culture Growth Based on an Inhibitory Effect of the Surrounding Biomass. *Bioprocess Biosyst. Eng.* **2021**, *44*, 1671–1684. [CrossRef]
40. Wang, Y.; Guo, W.; Yen, H.W.; Ho, S.H.; Lo, Y.C.; Cheng, C.L.; Ren, N.; Chang, J.S. Cultivation of *Chlorella vulgaris* JSC-6 with Swine Wastewater for Simultaneous Nutrient/COD Removal and Carbohydrate Production. *Bioresour. Technol.* **2015**, *198*, 619–625. [CrossRef]
41. Koletti, A.; Skliros, D.; Dervisi, I.; Roussis, A.; Flemetakis, E. Oxidative Stress Responses in Microalgae: Modern Insights into an Old Topic. *Appl. Microbiol.* **2025**, *5*, 37. [CrossRef]
42. Vijayan, J.; Wase, N.; Liu, K.; Morse, W.; Zhang, C.; Riekhof, W.R. ROS-Mediated Thylakoid Membrane Remodeling and Triacylglycerol Biosynthesis under Nitrogen Starvation in the Alga *Chlorella sorokiniana*. *Front. Plant Sci.* **2024**, *15*, 1418049. [CrossRef]
43. Ugya, A.Y.; Imam, T.S.; Li, A.; Ma, J.; Hua, X. Antioxidant Response Mechanism of Freshwater Microalgae Species to Reactive Oxygen Species Production: A Mini Review. *Chem. Ecol.* **2020**, *36*, 174–193. [CrossRef]
44. Alalawy, A.I.; Yang, Y.; Almutairi, F.M.; El Rabey, H.A.; Al-Duais, M.A.; Abomohra, A.; Salama, E.S. Freshwater Microalgae-Based Wastewater Treatment under Abiotic Stress. *AIMS Environ. Sci.* **2023**, *10*, 504–515. [CrossRef]
45. Dębowski, M.; Kisielewska, M.; Kazimierowicz, J.; Zieliński, M. Biophotolysis vs. Anaerobic Digestion—An Experimental Comparison of Two Pathways for Biohydrogen Production by *Tetraselmis subcordiformis*. *Phycology* **2025**, *5*, 74. [CrossRef]
46. Zieliński, M.; Barczak, Ł.; Rusanowska, P.; Kazimierowicz, J.; Dębowski, M. Comparison of Biohydrogen Production by *Tetraselmis subcordiformis* During Cultivation Using Soil-Less Agricultural Wastewater and Effluent from Microbial Fuel Cells. *Energies* **2024**, *17*, 5287. [CrossRef]
47. Zieliński, M.; Barczak, Ł.; Rusanowska, P.; Nowicka, A.; Dębowski, M. Microbial Fuel Cells as CO_2 Source in the Autotrophic Cultivation of the Green Microalgae *Tetraselmis subcordiformis*: Impact on Biomass Growth, Nutrient Removal, and Hydrogen Production. *Energies* **2025**, *18*, 874. [CrossRef]
48. Ugya, A.Y. The efficiency and antioxidant response of microalgae biofilm in the phycoremediation of wastewater resulting from tannery, textile, and dyeing activities. *Int. Aquat. Res.* **2021**, *13*, 289. [CrossRef]
49. Touloupakis, E.; Faraloni, C.; Silva Benavides, A.M.; Torzillo, G. Recent Achievements in Microalgal Photobiological Hydrogen Production. *Energies* **2021**, *14*, 7170. [CrossRef]
50. Uggetti, E.; Sialve, B.; Latrille, E.; Steyer, J.-P. Anaerobic digestate as substrate for microalgae culture: The role of ammonium concentration on the microalgae productivity. *Bioresour. Technol.* **2014**, *152*, 437–443. [CrossRef]
51. Jhouhanggir, D.I.P.; Pertiwiningrum, A.; Fitriyanto, N.A.; Suyono, E.A. Integrating anaerobic digestate effluent into microalgal systems for renewable biomass and wastewater treatment: Effects of dilution, c/n ratio, and growth modelling. *Results Eng.* **2025**, *27*, 106044. [CrossRef]
52. Scarponi, P.; Bonetto, A.; Bolzonella, D.; Astals, S.; Cavinato, C. Anaerobic Co-Digestion Effluent as Substrate for *Chlorella vulgaris* and *Scenedesmus obliquus* Cultivation. *Energies* **2020**, *13*, 4880. [CrossRef]
53. Zuliani, L.; Frison, N.; Jelic, A.; Fatone, F.; Bolzonella, D.; Ballottari, M. Microalgae Cultivation on Anaerobic Digestate of Municipal Wastewater, Sewage Sludge and Agro-Waste. *Int. J. Mol. Sci.* **2016**, *17*, 1692. [CrossRef]
54. Hu, Z.; Zhang, J.; Xie, H.; Li, S.; Wang, J.; Zhang, T. Effect of anoxic/aerobic phase fraction on N_2O emission in a sequencing batch reactor under low temperature. *Bioresour. Technol.* **2011**, *102*, 5486–5491. [CrossRef]
55. Cho, S.; Lee, N.; Park, S.; Yu, J.; Luong, T.T.; Oh, Y.-K.; Lee, T. Microalgae cultivation for bioenergy production using wastewaters from a municipal WWTP as nutritional sources. *Bioresour. Technol.* **2013**, *131*, 515–520. [CrossRef] [PubMed]
56. Zhang, Z.; Sun, D.; Cheng, K.W.; Chen, F. Investigation of Carbon and Energy Metabolic Mechanism of Mixotrophy in *Chromochloris zofingiensis*. *Biotechnol. Biofuels* **2021**, *14*, 36. [CrossRef] [PubMed]
57. Wu, X.; Jin, C.; Zhang, C.; Li, P.; Huang, J.J.; Wu, J.; Wu, J.; Hu, Z. Mixotrophic *Chlorella pyrenoidosa* Biofilm with Enhanced Biomass Production, Microalgal Activity, and Nutrient Removal from Nutrient-Rich Wastewater. *J. Environ. Sci.* **2025**, *157*, 366–377. [CrossRef] [PubMed]
58. Bhatnagar, A.; Chinnasamy, S.; Singh, M.; Das, K.C. Renewable Biomass Production by Mixotrophic Algae in the Presence of Various Carbon Sources and Wastewaters. *Appl. Energy* **2011**, *88*, 3425–3431. [CrossRef]
59. Miao, M.S.; Yao, X.D.; Shu, L.; Yan, Y.J.; Wang, Z.; Li, N.; Cui, X.-T.; Lin, Y.-M.; Kong, Q. Mixotrophic Growth and Biochemical Analysis of *Chlorella vulgaris* Cultivated with Synthetic Domestic Wastewater. *Int. Biodeterior. Biodegrad.* **2016**, *113*, 120–125. [CrossRef]

60. Nápoles-Armenta, J.; Romero-Soto, I.C.; Samaniego-Moreno, L.; Díaz-Tenorio, L.M.; Soto, L.A.L.; Mora-Orozco, C.D.L.; González Pérez, R.; Martínez-Orozco, E.; García-Gómez, C.; Pérez-Valencia, L.I. Advanced Municipal Wastewater Treatment and Bioproduct Generation via Optimized Autotrophic and Mixotrophic Microalgal Cultivation. *Sustainability* **2025**, *17*, 6539. [CrossRef]
61. Goswami, R.K.; Agrawal, K.; Mehariya, S.; Rajagopal, R.; Karthikeyan, O.P.; Verma, P. Development of Economical and Sustainable Cultivation System for Biomass Production and Simultaneous Treatment of Municipal Wastewater Using *Tetraselmis indica* BDUG001. *Environ. Technol.* **2023**, 1–21. [CrossRef]
62. Michels, M.H.A.; Vaskoska, M.; Vermuë, M.H.; Wijffels, R.H. Growth of *Tetraselmis suecica* in a tubular photobioreactor on wastewater from a fish farm. *Water Res.* **2014**, *65C*, 290–296. [CrossRef]
63. Goswami, R.K.; Agrawal, K.; Mehariya, S.; Verma, P. Current Perspective on Wastewater Treatment Using Photobioreactor for *Tetraselmis sp.*: An Emerging and Foreseeable Sustainable Approach. *Environ. Sci. Pollut. Res.* **2022**, *29*, 61905–61937. [CrossRef]
64. Amit, G.; Ghosh, U.K.; Gautam, R.; Jaiswal, A.; Pandey, S. Phycoremediation of Dairy Wastewater and Biodiesel Production Using Marine Microalgae *Tetraselmis indica*. In *Advances in Functional and Smart Materials: Select Proceedings of ICFMMP 2021*; Springer: Singapore, 2021. [CrossRef]
65. Schmidt, J.J.; Gagnon, G.A.; Jamieson, R.C. Microalgae Growth and Phosphorus Uptake in Wastewater under Simulated Cold Region Conditions. *Ecol. Eng.* **2016**, *95*, 588–593. [CrossRef]
66. Su, Y. Revisiting Carbon, Nitrogen, and Phosphorus Metabolisms in Microalgae for Wastewater Treatment. *Sci. Total Environ.* **2021**, *762*, 144590. [CrossRef] [PubMed]
67. Dyhrman, S.T.; Jenkins, B.D.; Rynearson, T.A.; Saito, M.A.; Mercier, M.L.; Alexander, H.; Whitney, L.P.; Drzewianowski, A.; Bulygin, V.V.; Bertrand, E.M.; et al. The Transcriptome and Proteome of the Diatom *Thalassiosira pseudonana* Reveal a Diverse Phosphorus Stress Response. *PLoS ONE* **2012**, *7*, e33768. [CrossRef] [PubMed]
68. Solovchenko, A.E.; Ismagulova, T.T.; Lukyanov, A.A.; Svetlana, G.V.; Konyukhov, I.V.; Pogosyan, S.I.; Lobakova, E.S.; Gorelova, O.A. Luxury Phosphorus Uptake in Microalgae. *J. Appl. Phycol.* **2019**, *31*, 2755–2770. [CrossRef]
69. Wang, J.H.; Zhang, T.Y.; Dao, G.H.; Xu, X.-Q.; Wang, X.-X.; Hu, H.-Y. Microalgae-Based Advanced Municipal Wastewater Treatment for Reuse in Water Bodies. *Appl. Microbiol. Biotechnol.* **2017**, *101*, 2659–2675. [CrossRef]
70. Ge, H.; Li, J.; Chen, P.; Chang, Z.; Shen, M.; Zhao, F. Cultivation of Green Algae *Platymonas helgolandica* in Rearing Water Enhances the Growth Performance and Resistance of *Litopenaeus vannamei* against *Vibrio parahaemolyticus* Infection. *Aquac. Int.* **2017**, *25*, 1279–1290. [CrossRef]
71. Jia, H.; Yuan, Q. Removal of Nitrogen from Wastewater Using Microalgae and Microalgae–Bacteria Consortia. *Cogent Environ. Sci.* **2016**, *2*, 1275089. [CrossRef]
72. Giordano, M.; Raven, J.A. Nitrogen and Sulfur Assimilation in Plants and Algae. *Aquat. Bot.* **2014**, *118*, 45–61. [CrossRef]
73. Turon, V.; Baroukh, C.; Trably, E.; Latrille, E.; Fouilland, E.; Steyer, J.-P. Use of Fermentative Metabolites for Heterotrophic Microalgae Growth: Yields and Kinetics. *Bioresour. Technol.* **2015**, *175*, 342–349. [CrossRef] [PubMed]
74. Heredia-Arroyo, T.; Wei, W.; Ruan, R.; Hu, B. Mixotrophic Cultivation of *Chlorella vulgaris* and Its Potential Application for Oil Accumulation from Non-Sugar Materials. *Biomass Bioenergy* **2011**, *35*, 2245–2253. [CrossRef]
75. Chen, F.; Johns, M.R. Substrate Inhibition of *Chlamydomonas reinhardtii* by Acetate in Heterotrophic Culture. *Process Biochem.* **1994**, *29*, 245–252. [CrossRef]
76. Perchikov, R.; Cheliukanov, M.; Plekhanova, Y.; Tarasov, S.; Kharkova, A.; Butusov, D.; Arlyapov, V.; Nakamura, H.; Reshetilov, A. Microbial Biofilms: Features of Formation and Potential for Use in Bioelectrochemical Devices. *Biosensors* **2024**, *14*, 302. [CrossRef]
77. Nosek, D.; Mikołajczyk, T.; Cydzik-Kwiatkowska, A. Enhancing microbial fuel cell performance: Anode modification with reduced graphene oxide and iron (III) for improved electricity generation. *Clean. Technol. Environ. Policy* **2024**, *26*, 4095–4112. [CrossRef]
78. Mei, X.; Lu, B.; Yan, C.; Gu, J.; Ren, N.; Ren, Z.J.; Xing, D. The interplay of active energy harvesting and wastewater organic loading regulates fermentation products and microbiomes in microbial fuel cells. *Resour. Conserv. Recycl.* **2022**, *183*, 106366. [CrossRef]
79. Ramírez-Vargas, C.A.; Prado, A.; Arias, C.A.; Carvalho, P.N.; Esteve-Núñez, A.; Brix, H. Microbial Electrochemical Technologies for Wastewater Treatment: Principles and Evolution from Microbial Fuel Cells to Bioelectrochemical-Based Constructed Wetlands. *Water* **2018**, *10*, 1128. [CrossRef]
80. Mahto, K.U.; Das, S. Electroactive biofilm communities in microbial fuel cells for the synergistic treatment of wastewater and bioelectricity generation. *Crit. Rev. Biotechnol.* **2025**, *45*, 434–453. [CrossRef]
81. Pandit, S.; Savla, N.; Sonawane, J.M.; Sani, A.M.; Gupta, P.K.; Mathuriya, A.S.; Rai, A.K.; Jadhav, D.A.; Jung, S.P.; Prasad, R. Agricultural Waste and Wastewater as Feedstock for Bioelectricity Generation Using Microbial Fuel Cells: Recent Advances. *Fermentation* **2021**, *7*, 169. [CrossRef]
82. Isanta-Navarro, J.; Peoples, L.M.; Bras, B.; Church, M.J.; Elser, J.J. Elemental and Macromolecular Plasticity of *Chlamydomonas Reinhardtii (Chlorophyta)* in Response to Resource Limitation and Growth Rate. *J. Phycol.* **2024**, *60*, 418–431. [CrossRef]

83. Bora, A.; Rajan, A.S.T.; Ponnuchamy, K.; Muthusamy, G.; Alagarsamy, A. Microalgae to bioenergy production: Recent advances, influencing parameters, utilization of wastewater–A critical review. *Sci. Total Environ.* **2024**, *946*, 174230. [CrossRef]
84. Hillebrand, H.; Steinert, G.; Boersma, M.; Malzahn, A.; Meunier, C.L.; Plum, C.; Ptacnik, R. Golman Revisited: Faster-Growing Phytoplankton Has Lower N:P and Lower Stoichiometric Flexibility. *Limnol. Oceanogr.* **2013**, *58*, 2076–2088. [CrossRef]
85. Loladze, I.; Elser, J.J. The Origins of the Redfield Nitrogen-to-Phosphorus Ratio Are in a Homoeostatic Protein-to-rRNA Ratio. *Ecol. Lett.* **2011**, *14*, 244–250. [CrossRef] [PubMed]
86. Bi, R.; Arndt, C.; Sommer, U. Stoichiometric Responses of Phytoplankton Species to the Interactive Effect of Nutrient Supply Ratios and Growth Rates. *J. Phycol.* **2012**, *48*, 539–549. [CrossRef] [PubMed]
87. Ekpan, F.M.; Ori, M.O.; Samuel, H.S. Effects of Environmental Factors and Nutrient Availability on the Biochemical Composition of Algae for Biofuel Production. *Discov. Appl. Sci.* **2025**, *7*, 1209. [CrossRef]
88. Ledda, C.; Idà, A.; Allemand, D.; Mariani, P.; Adani, F. Production of wild Chlorella sp. cultivated in digested and membrane-pretreated swine manure derived from a full-scale operation plant. *Algal Res.* **2015**, *12*, 68–73. [CrossRef]
89. Abu Hajar, H.A.; Riefler, R.G.; Stuart, B.J. Cultivation of *Scenedesmus dimorphus* using anaerobic digestate as a nutrient medium. *Bioprocess Biosyst. Eng.* **2017**, *40*, 1197–1207. [CrossRef]
90. de Farias Silva, C.E.; Sforza, E.; Bertucco, A. Stability of Carbohydrate Production in Continuous Microalgal Cultivation under Nitrogen Limitation: Effect of Irradiation Regime and Intensity on *Tetradesmus Obliquus*. *J. Appl. Phycol.* **2018**, *30*, 261–270. [CrossRef]
91. Sun, Q.; Zhang, X.; Zhang, X. Impact of Natural Microorganisms on the Removal of COD and the Cells Activity of *Chlorella* sp. in Wastewater. *Water* **2023**, *15*, 3544. [CrossRef]
92. Cheng, D.; He, Q. Assessment of Environmental Stresses for Enhanced Microalgal Biofuel Production–An Overview. *Front. Energy Res.* **2014**, *2*, 26. [CrossRef]
93. Plouviez, M.; Abyadeh, M.; Hasan, M.; Mirzaei, M.; Paulo, J.A.; Guieysse, B. The Proteome of *Chlamydomonas reinhardtii* during Phosphorus Depletion and Repletion. *Algal Res.* **2023**, *71*, 103037. [CrossRef]
94. Suárez Quintana, W.H.; García-Rico, R.O.; García-Martínez, J.B.; Urbina-Suarez, N.A.; López-Barrera, G.L.; Barajas-Solano, A.F.; Zuorro, A. Enhancement of Metabolite Production in High-Altitude Microalgal Strains by Optimized C/N/P Ratio. *Appl. Sci.* **2022**, *12*, 6779. [CrossRef]
95. Huang, X.-L.; Zhuang, Y.-Q.; Xiong, Y.-Y.; Li, D.-W.; Ou, L.-J. Efficient Modulation of Cellular Phosphorus Components in Response to Phosphorus Deficiency in the Dinoflagellate *Karenia mikimotoi*. *Appl. Environ. Microbiol.* **2023**, *89*, e0086723. [CrossRef] [PubMed]
96. Qari, H.A.; Al-Shaeri, M.A.; Oves, M. Effect of Phosphorus Deprivation on Fatty Acid Synthesis in *Scenedesmus subspicatus* Microalgae from Rostherne Mere. *Fuels* **2024**, *5*, 910–926. [CrossRef]
97. Baiee, M.A.; Salman, J.M. Effect of Phosphorus Concentration and Light Intensity on Protein Content of Microalga *Chlorella vulgaris*. *Mesopotamian Environ. J.* **2016**, *2*, 75–86.
98. Hippler, M.; Khosravitabar, F. Light-Driven H_2 Production in *Chlamydomonas reinhardtii*: Lessons from Engineering of Photosynthesis. *Plants* **2024**, *13*, 2114. [CrossRef]
99. Hwang, J.H.; Kim, H.C.; Choi, J.A.; Abou-Shanab, R.A.I.; Dempsey, B.A.; Regan, J.M.; Kim, J.R.; Song, H.; Nam, I.-H.; Kim, S.-N.; et al. Photoautotrophic Hydrogen Production by Eukaryotic Microalgae under Aerobic Conditions. *Nat. Commun.* **2014**, *5*, 3234. [CrossRef]
100. Nagy, V.; Podmaniczki, A.; Vidal-Meireles, A.; Tengölics, R.; Kovács, L.; Rákhely, G.; Scoma, A.; Tóth, S.Z. Water-Splitting-Based, Sustainable and Efficient H_2 Production in Green Algae as Achieved by Substrate Limitation of the Calvin-Benson-Bassham Cycle. *Biotechnol. Biofuels* **2018**, *11*, 69. [CrossRef]
101. Liran, O.; Semyatich, R.; Milrad, Y.; Eilenberg, H.; Weiner, I.; Yacoby, I. Microoxic Niches within the Thylakoid Stroma of Air-Grown *Chlamydomonas reinhardtii* Protect [FeFe]-Hydrogenase and Support Hydrogen Production under Fully Aerobic Environment. *Plant Physiol.* **2016**, *172*, 264–271. [CrossRef]
102. Wang, X.; Li, S.-Y.; Chen, Y.; Chen, Y.-P.; Guo, J.-S.; Liu, S.-Y.; Yan, P. New Insights into Microalgal Photobiological Hydrogen Production: Potential Role of Aggregation Forms in Modulating the Hydrogenase Activity and Metabolic Properties of Microalgae during Hydrogen Production. *Chem. Eng. J.* **2024**, *500*, 156802. [CrossRef]
103. Koo, J.; Swartz, J.R. System Analysis and Improved [FeFe] Hydrogenase O_2 Tolerance Suggest Feasibility for Photosynthetic H_2 Production. *Metab. Eng.* **2018**, *49*, 21–27. [CrossRef]
104. Seibert, M.; King, P.W.; Posewitz, M.C.; Melis, A.; Ghirardi, M.L. Photosynthetic water-splitting for hydrogen production. In *Bioenergy*; ASM Press: Washington, DC, USA, 2008; pp. 273–291. [CrossRef]
105. Zhang, B.; Wu, J.; Meng, F. Adaptive Laboratory Evolution of Microalgae: A Review of the Regulation of Growth, Stress Resistance, Metabolic Processes, and Biodegradation of Pollutants. *Front. Microbiol.* **2021**, *12*, 737248. [CrossRef]
106. Hallenbeck, P.C.; Abo-Hashesh, M.; Ghosh, D. Strategies for improving biological hydrogen production. *Bioresour. Technol.* **2012**, *110*, 1–9. [CrossRef]

107. Touloupakis, E.; Faraloni, C.; Silva Benavides, A.M.; Masojidek, J.; Torzillo, G. Sustained photobiological hydrogen production by *Chlorella vulgaris* without nutient starvation. *Int. J. Hydrogen Energy* **2021**, *46*, 3684–3694. [CrossRef]
108. Daneshvar, E.; Zarrinmehr, M.J.; Hashtjin, A.M.; Farhadian, O.; Bhatnagar, A. Versatile applications of freshwater and marine water microalgae in dairy wastewater treatment, lipid extraction and tetracycline biosorption. *Bioresour. Technol.* **2018**, *268*, 523–530. [CrossRef] [PubMed]
109. Ruiz-Marin, A.; Canedo-López, Y.; Chávez-Fuentes, P. Biohydrogen production by Chlorella vulgaris and Scenedesmus obliquus immobilized cultivated in artificial wastewater under different light quality. *AMB Express* **2020**, *10*, 191. [CrossRef] [PubMed]
110. Dębowski, M.; Dudek, M.; Zieliński, M.; Nowicka, A.; Kazimierowicz, J. Microalgal Hydrogen Production in Relation to Other Biomass-Based Technologies—A Review. *Energies* **2021**, *14*, 6025. [CrossRef]
111. Jiao, H.; Tsigkou, K.; Elsamahy, T.; Pispas, K.; Sun, J.; Manthos, G.; Schagerl, M.; Sventzouri, E.; Al-Tohamy, R.; Kornaros, M.; et al. Recent Advances in Sustainable Hydrogen Production from Microalgae: Mechanisms, Challenges, and Future Perspectives. *Ecotoxicol. Environ. Saf.* **2024**, *270*, 115908. [CrossRef]
112. El-Dalatony, M.M.; Zheng, Y.; Ji, M.K.; Li, X.; Salama, E.S. Metabolic Pathways for Microalgal Biohydrogen Production: Current Progress and Future Prospectives. *Bioresour. Technol.* **2020**, *318*, 124253. [CrossRef]
113. Ardo, F.M.; Lim, J.W.; Ramli, A.; Lam, M.K.; Kiatkittipong, W.; Abdelfattah, E.A.; Shahid, M.K.; Usman, A.; Wongsakulphasatch, S.; Sahrin, N.T. A Review in Redressing Challenges to Produce Sustainable Hydrogen from Microalgae for Aviation Industry. *Fuel* **2022**, *330*, 125646. [CrossRef]
114. Arimbrathodi, S.P.; Javed, M.A.; Hamouda, M.A.; Hassan, A.A.; Ahmed, M.E. BioH_2 Production Using Microalgae: Highlights on Recent Advancements from a Bibliometric Analysis. *Water* **2023**, *15*, 185. [CrossRef]
115. Ahmed, S.F.; Mofijur, M.; Nahrin, M.; Chowdhury, S.N.; Nuzhat, S.; Alherek, M.; Rafa, N.; Ong, H.C.; Nghiem, L.D.; Mahlia, T.M.I. Biohydrogen Production from Wastewater-Based Microalgae: Progresses and Challenges. *Int. J. Hydrogen Energy* **2021**, *47*, 37321–37342. [CrossRef]

Disclaimer/Publisher's Note: The statements, opinions and data contained in all publications are solely those of the individual author(s) and contributor(s) and not of MDPI and/or the editor(s). MDPI and/or the editor(s) disclaim responsibility for any injury to people or property resulting from any ideas, methods, instructions or products referred to in the content.